UVB Exposure Prevents Atherosclerosis by Regulating Immunoinflammatory Responses

Naoto Sasaki, Tomoya Yamashita, Kazuyuki Kasahara, Atsushi Fukunaga, Tomoyuki Yamaguchi, Takuo Emoto, Keiko Yodoi, Takuya Matsumoto, Kenji Nakajima, Tomoyuki Kita, Masafumi Takeda, Taiji Mizoguchi, Tomohiro Hayashi, Yoshihiro Sasaki, Mayumi Hatakeyama, Kumiko Taguchi, Ken Washio, Shimon Sakaguchi, Bernard Malissen, Chikako Nishigori, Ken-ichi Hirata

Objective—UVB irradiation is an established treatment for immunoinflammatory cutaneous disorders and has been shown to suppress cutaneous and systemic inflammatory diseases through modulation of the adaptive immune response. However, it remains unknown whether UVB irradiation prevents an immunoinflammatory disease of arteries such as atherosclerosis.

Approach and Results—Here, we show that UVB exposure inhibits the development and progression of atherosclerosis in atherosclerosis-prone mice by expanding and enhancing the functional capacity of $CD4^+$ forkhead box $P3^+$ regulatory T cells and regulating proatherogenic T-cell responses. Experimental studies in Langerhans cell–depleted mice revealed that epidermal Langerhans cells play a critical role in UVB-dependent induction of $CD4^+$ forkhead box $P3^+$ regulatory T cells, suppression of proatherogenic T-cell responses, and prevention of atherosclerotic plaque development.

Conclusions—Our findings suggest the skin immune system as a novel therapeutic target for atherosclerosis and provide a novel strategy for the treatment and prevention of atherosclerosis. **(*Arterioscler Thromb Vasc Biol*. 2017;37:66-74. DOI: 10.1161/ATVBAHA.116.308063.)**

Key Words: atherosclerosis ■ immunology ■ inflammation ■ lymphocytes ■ ultraviolet rays

Atherosclerotic disease including ischemic heart disease and stroke is a major cause of mortality in developed countries. Atherosclerosis involves chronic inflammation of the arterial wall.[1] Innate and adaptive immune responses contribute to the development and rupture of unstable atherosclerotic plaques and subsequent thrombotic arterial occlusion, leading to fatal clinical events. Chronic vascular inflammation via T-cell–mediated immune responses is well known to play an important role in atherogenesis.[2] Recent experimental studies from several independent groups indicated that several subsets of regulatory T cells (Tregs) including forkhead box P3 (Foxp3)–expressing Tregs, which actively mediate immunologic tolerance,[3] play a role in preventing atherosclerosis by dampening proatherogenic T-cell responses or modulating lipoprotein metabolism,[4–6] revealing the importance of the balance between proatherogenic T cells and atheroprotective Tregs in the control of atherosclerotic diseases.[7] There is also increasing clinical evidence showing the dysregulation of this balance in human coronary atherosclerotic disease.[8,9]

See accompanying editorial on page 7

It has long been known that UV irradiation critically affects the immune system. Numerous studies in the field of photoimmunology have reported that UV irradiation, in particular UVB, induces immunosuppression and dampens inflammatory reactions.[10] For evaluation of biological functions of UVB, several studies used mouse contact hypersensitivity model, in which UVB suppresses hapten-mediated contact hypersensitivity in an antigen-specific manner.[11] Interestingly, this phenomenon has been shown to be associated with generation of antigen-specific Tregs.[10] Langerhans cells (LCs) are the major antigen-presenting cells in the skin,[12] where the immune system is constantly stimulated by the environment and they regulate adaptive immune responses in response to various stimuli. Recent studies suggest that epidermal LCs

Received on: June 28, 2016; final version accepted on: October 10, 2016.

From the Division of Cardiovascular Medicine, Department of Internal Medicine (N.S., T. Yamashita., K.K., T.E., K.Y., T. Matsumoto, K.N., T.K., M.T., T. Mizoguchi, T.H., Y.S., K.-i.H.) and Division of Dermatology, Department of Internal Related (A.F., M.H., K.T., K.W., C.N.), Kobe University Graduate School of Medicine, Japan; Department of Medical Pharmaceutics, Kobe Pharmaceutical University, Japan (N.S.); Department of Single Molecule Imaging (T. Yamaguchi) and Department of Experimental Immunology (S.S.), World Premier International Immunology Frontier Research Center, Osaka University, Japan; Department of Cell Growth and Differentiation, Center for iPS Cell Research and Application (CiRA), Kyoto University, Japan (M.T.); and Centre d'Immunologie de Marseille-Luminy and the Centre d'Immunophénomique, UM2 Aix-Marseille Université, Marseille, France (B.M.).

The online-only Data Supplement is available with this article at http://atvb.ahajournals.org/lookup/suppl/doi:10.1161/ATVBAHA.116.308063/-/DC1.

Correspondence to Naoto Sasaki, MD, PhD, Department of Medical Pharmaceutics, Kobe Pharmaceutical University, 4-19-1, Motoyamakita-machi, Higashinada-ku, Kobe, 658-8558, Japan. E-mail n-sasaki@kobepharma-u.ac.jp; or Tomoya Yamashita, MD, PhD, Division of Cardiovascular Medicine, Department of Internal Medicine, Kobe University Graduate School of Medicine, 7-5-1, Kusunoki-cho, Chuo-ku, Kobe, 650-0017, Japan. E-mail tomoya@med.kobe-u.ac.jp

Nonstandard Abbreviations and Acronyms	
Apoe	apolipoprotein E
DC	dendritic cell
DT	diphtheria toxin
Foxp3	forkhead box P3
IFN	interferon
IL	interleukin
LC	Langerhans cell
LN	lymph node
Th	T helper type
Treg	regulatory T cell

undergo morphological changes and alter their function during UVB-induced immunosuppression.[13,14]

Despite advances in our understanding of the chronic immunoinflammatory nature of atherosclerosis, therapeutics aimed to intervene inflammation or immune system remains to be implemented in clinical practice. UVB-based phototherapy is the first-line treatment for immunoinflammatory cutaneous disorders such as psoriasis in humans without serious side effects.[15] Here, we investigated the effect of UVB irradiation on atherosclerosis and its underlying mechanisms in hypercholesterolemic mice. Our findings provide first evidence that UVB exposure inhibits the development and progression of atherosclerosis. Using hypercholesterolemic LC-depleted mice, we clearly demonstrated that epidermal LCs play a critical role in UVB-dependent induction of $CD4^+Foxp3^+$ Tregs, suppression of proatherogenic T-cell responses, and prevention of atherosclerotic plaque development. Our data suggest that UVB-based modulation of the skin immune system for inducing atheroprotective Tregs may be an attractive approach to treat and prevent atherosclerosis.

Materials and Methods

Materials and Methods are available in the online-only Data Supplement.

Results

UVB Irradiation Inhibits the Initiation and Progression of Atherosclerotic Plaque Formation in Atherosclerotic Mice

To study the effect of UVB irradiation on the development of atherosclerosis, apolipoprotein E–deficient ($Apoe^{-/-}$) mice were irradiated with 2 or 5 kJ/m^2 UVB once weekly for 14 weeks. During the experiments, severe adverse effects such as skin cancer or skin inflammation were not observed following UVB exposure. UVB irradiation did not affect body weight and plasma lipid profile (Table I in the online-only Data Supplement). We found a significant increase in biologically active 1,25-dihydroxyvitamin D plasma levels, whereas plasma levels of circulating storage form 25-hydroxyvitamin D were unaffected (Table I in the online-only Data Supplement). At 20 weeks of age, the mice were euthanized and atherosclerotic lesions were evaluated. UVB-irradiated mice showed a marked reduction in atherosclerotic lesion formation in the aortic root compared with control mice. Mean±SD of mean atherosclerotic lesion area in the aortic sinus was $2.94\times10^5\pm0.98\times10^5$ μm^2 in control nonirradiated mice, $1.95\times10^5\pm0.69\times10^5$ μm^2 in 2 kJ/m^2 UVB-irradiated mice (P=0.0112, versus controls), and $1.85\times10^5\pm0.65\times10^5$ μm^2 in 5 kJ/m^2 UVB-irradiated mice (P=0.0065, versus controls), as shown in Figure 1A. In parallel with the cross-sectional studies, en face analysis of thoracoabdominal aortas revealed a significant reduction in aortic plaque burden at 20 weeks in 5 kJ/m^2 UVB-irradiated mice (mean±SD, 2.62±0.85%; P=0.0041 versus controls) compared with control mice (mean±SD, 5.13±1.84%; Figure 1B). There was a tendency toward reduction in atherosclerotic plaque even in 2 kJ/m^2 UVB-irradiated mice (mean±SD, 3.63±1.56%; P=0.1023 versus controls; Figure 1B).

To determine the effects of UVB irradiation on plaque component, we next performed immunohistochemical studies of atherosclerotic lesions in the aortic sinus. Interestingly, the atherosclerotic lesions of UVB-irradiated mice showed a marked reduction in the accumulation of macrophages and a significant decrease in $CD4^+$ T-cell infiltration (Figure 1C) compared with control mice. The number of Tregs in the atherosclerotic lesions was not significantly affected by UVB irradiation (Figure IA in the online-only Data Supplement), which is in line with the results of real-time reverse transcription-PCR analysis showing no changes in the mRNA expression of aortic Treg-associated molecules after UVB exposure, except for the increased mRNA expression of cytotoxic T lymphocyte–associated antigen-4, a critical molecule for Treg-mediated suppression (Figure IB in the online-only Data Supplement). Collagen content in the aortic sinus plaques was not affected by UVB irradiation (Figure II in the online-only Data Supplement). These results suggest that UVB irradiation reduces intraplaque accumulation of inflammatory cells, which may lead to decreased lesion development.

Next, we examined the effect of UVB irradiation on the progression of established atherosclerotic plaques in $Apoe^{-/-}$ mice. Twenty-week-old female $Apoe^{-/-}$ mice, which have already suffered from atherosclerosis as shown in Figure 1A and 1B, were irradiated with 2 or 5 kJ/m^2 UVB once weekly for 10 weeks and euthanized at 30 weeks of age, and atherosclerotic lesions were assessed. Suppression of plaque progression was only observed in 5 kJ/m^2 UVB-irradiated mice (Figure III in the online-only Data Supplement).

UVB Irradiation Expands $CD4^+Foxp3^+$ Tregs With Potent Suppressive Activity and Suppresses Proatherogenic T-Cell Responses

Next, we determined the mechanisms by which UVB irradiation prevents atherosclerosis by assessing the changes in systemic immune responses including $CD4^+Foxp3^+$ Tregs after UVB exposure. $Apoe^{-/-}$ mice were irradiated with 2 or 5 kJ/m^2 UVB once weekly for 3 weeks. Lymphoid cells from skin-draining lymph nodes (LNs) and spleen were prepared and analyzed by flow cytometry. UVB irradiation significantly increased the frequency and numbers of $CD4^+Foxp3^+$ Tregs in the skin-draining LNs of hypercholesterolemic $Apoe^{-/-}$ mice (Figure 2A). In addition, an increase in frequency of $CD4^+Foxp3^+$ Tregs was also observed in the spleen of UVB-irradiated mice (Figure 2A). Similar results were obtained for

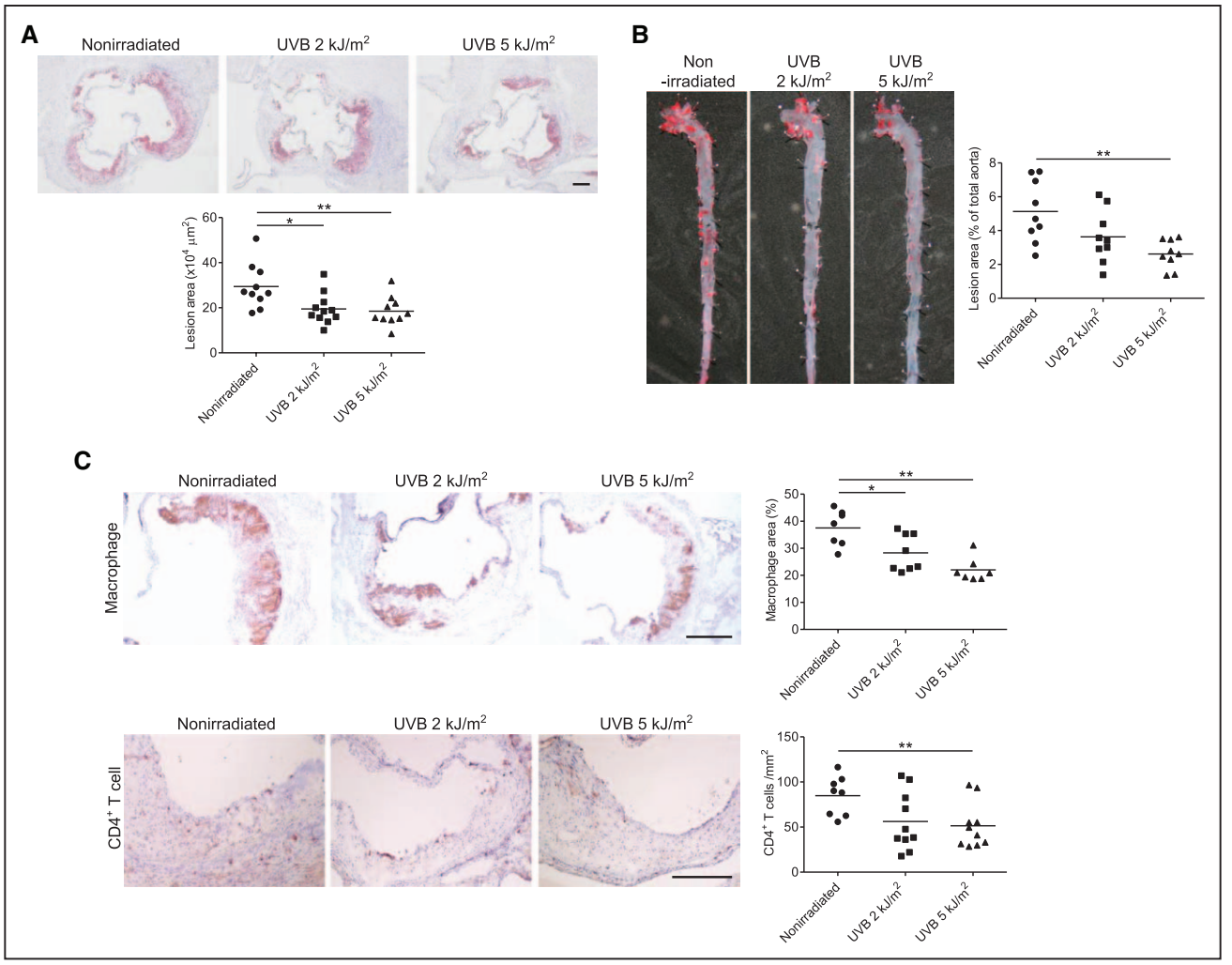

Figure 1. UVB irradiation inhibits the development of atherosclerosis and plaque inflammation. Six-week-old female apolipoprotein E–deficient (*Apoe*$^{-/-}$) mice were irradiated with 2 or 5 kJ/m^2 UVB once weekly for 14 wk and killed at 20 wk of age, and atherosclerotic lesions were assessed. Nonirradiated mice served as controls. **A**, Representative photomicrographs of Oil-red-O staining and quantitative analysis of atherosclerotic lesion area in the aortic sinus of UVB-irradiated (n=11 for 2 kJ/m^2 UVB; n=10 for 5 kJ/m^2 UVB) or nonirradiated mice (n=10). **B**, Representative photomicrographs of Oil-red-O staining and quantitative analysis of atherosclerotic lesion area in the aortas of UVB-irradiated or nonirradiated mice (n=9 per group). **C**, Effects of UVB irradiation on atherosclerotic phenotype. Representative sections and quantitative analyses of MOMA-2$^+$ macrophages and CD4$^+$ T cells in the aortic sinus. n=7 to 10 per group. Black bars represent 200 μm. Data points represent individual animals. Horizontal bars represent means. *P<0.05, **P<0.01, Mann–Whitney U test.

CD4$^+$CD25^{high}Foxp3$^+$ Tregs (Figure IV in the online-only Data Supplement).

To determine the function of UVB-induced Tregs, we investigated the effects of UVB irradiation on the expression of Treg-associated molecules in CD4$^+$Foxp3$^+$ Tregs in LNs and spleen using flow cytometry. Interestingly, UVB-induced CD4$^+$Foxp3$^+$ Tregs expressed higher levels of typical Treg markers including cytotoxic T lymphocyte–associated antigen-4 and CD103, while CD25 and glucocorticoid-induced tumor necrosis factor receptor family–related gene/protein were expressed at equivalent levels to those from nonirradiated mice (Figure 2B and 2C). Among various suppression mechanisms,[3] cytotoxic T lymphocyte–associated antigen-4 is known to be constitutively expressed by CD4$^+$Foxp3$^+$ Tregs as a core mechanism for Treg-mediated suppression.[16] Therefore, we examined a possibility that UVB treatment might enhance the suppressive function in each Treg. The in vitro suppression assay revealed that Tregs from UVB-irradiated mice had higher suppressive capacity compared with those from controls (Figure 2D). Dendritic cells (DCs) express costimulatory molecules such as B7-1 (CD80) and B7-2 (CD86) that bind to receptors on the T cells simultaneously with antigen recognition, which leads to T-cell activation. Downregulation of CD80 and CD86 expression on DCs by cytotoxic T lymphocyte–associated antigen-4 is reported to be a key mechanism for Treg-mediated suppression.[16] Interestingly, effector T-cell–dependent upregulation of CD80 and CD86 expression on splenic CD11c$^+$ DCs was suppressed by cocultured Tregs, and UVB irradiation enhanced the suppression (Figure 2E).

To determine whether induction of CD4$^+$Foxp3$^+$ Tregs by UVB irradiation affects T-cell responses, we examined cytokine secretion from T cells by ELISA and intracellular cytokine staining. Importantly, splenic lymphocytes from UVB-irradiated mice stimulated with concanavalin A in vitro secreted less proatherogenic T helper type 1 (Th1)–related cytokine interferon (IFN)-γ than those from controls, whereas no

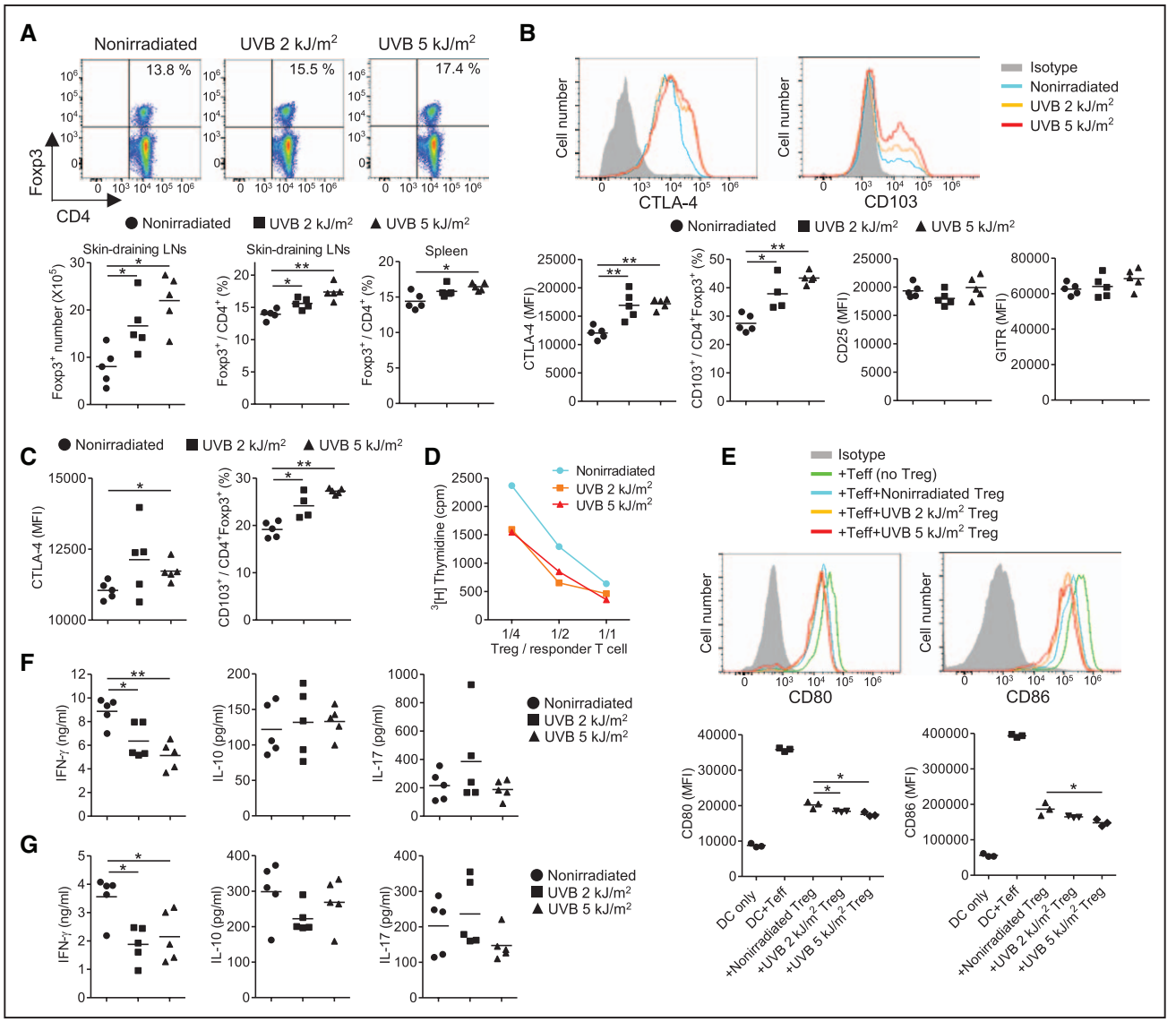

Figure 2. UVB irradiation expands CD4⁺ forkhead box P3 (Foxp3)⁺ regulatory T cells (Tregs) with potent suppressive activity and suppresses proatherogenic T-cell responses. Apolipoprotein E–deficient (*Apoe*$^{-/-}$) mice were irradiated with 2 or 5 kJ/m² UVB once weekly for 3 wk. Nonirradiated mice served as controls. Three (**A**–**C**, **F**) or 4 (**D** and **E**) d after the last UVB irradiation, lymphoid cells from skin-draining lymph nodes (LNs) and spleen were prepared. **A**, Representative results of Foxp3 expression in LN CD4⁺ T cells assessed by flow cytometry. The graphs represent total numbers of LN Foxp3⁺ Tregs and percentage of Foxp3⁺ Tregs within the LN and spleen CD4⁺ population. n=5 per group. **B** and **C**, The expression levels of Treg-associated markers were analyzed gating on CD4⁺Foxp3⁺ Tregs in LNs (**B**) and spleen (**C**). Histograms show mean fluorescence intensity (MFI). n=4 to 5 per group. **D**, LN CD4⁺CD25⁺ Tregs from UVB-irradiated or control mice were cocultured with responder CD4⁺CD25⁻ T cells at the indicated ratios and their suppressive function was assessed by [³H]-thymidine incorporation. **E**, CD80 and CD86 expression of live splenic CD11c⁺ dendritic cells (DCs) after 2-d coculture with effector CD4⁺CD25⁻ T cells (Teffs), or a mix of CD4⁺CD25⁺ Tregs and CD4⁺CD25⁻ Teffs in the presence of anti-CD3 antibody. Histograms show MFI. Data are results of triplicate wells. **F**, Splenocytes from UVB-irradiated or control mice were stimulated with concanavalin A in vitro. Cytokine production from splenic lymphocytes was examined by ELISA. n=5 per group. **G**, To examine the effect of long-term UVB irradiation on cytokine production from splenic lymphocytes, 6-wk-old *Apoe*$^{-/-}$ mice were irradiated with 2 or 5 kJ/m² UVB once weekly for 14 wk. Cytokine production from splenic lymphocytes was measured as described above. n=5 per group. Data are representative of 2 independent experiments (**A**–**F**). Data points represent individual animals (**A**–**C**, **F**, **G**). Horizontal bars represent means (**A**–**C**, **E**–**G**). **P*<0.05; ***P*<0.01; Mann–Whitney *U* test (**A**–**C**, **F**, **G**) and 2-tailed Student *t* test (**E**). CTLA-4 indicates cytotoxic T lymphocyte–associated antigen-4; and GITR, glucocorticoid-induced tumor necrosis factor receptor family–related gene/protein.

differences in Th2 or Treg-related cytokine interleukin (IL)-10 and Th17-related cytokine IL-17 were observed (Figure 2F). The production of Th2-related cytokine IL-4 was below detection levels in all groups. Similar results were obtained after long-term UVB irradiation (Figure 2G). UVB irradiation did not affect the fractions of IFN-γ–, IL-4–, IL-10–, or IL-17–producing CD4⁺ T cells (Figure VA in the online-only Data Supplement) or other splenic immune cell subsets except for CD11c⁺ DCs, which were slightly decreased in UVB-irradiated mice (Figure VB in the online-only Data Supplement). There were no differences in the expression of CD80 and CD86 on splenic CD11c⁺ DCs between UVB-irradiated and nonirradiated mice (Figure VB in the online-only Data Supplement), which may be because of compensatory mechanisms. Taken

together, these results indicate that UVB irradiation resulted in a significant increase in CD4⁺Foxp3⁺ Tregs with potent suppressor function, which may lead to suppression of pathogenic Th1 immune responses.

Epidermal LCs Are Critically Involved in UVB-Dependent Induction of CD4⁺Foxp3⁺ Tregs and Suppression of Proatherogenic T-Cell Responses

The important role of epidermal-resident antigen-presenting LCs in UVB-induced immune suppression has been reported,[13,14] but it is still unclear whether they are essential for Treg induction on UVB exposure. LC might play a role in UVB-mediated atherosclerosis reduction although no reports have directly approached this possibility to date. It is reported that UVB exposure triggers the migration of LCs from the skin to the draining LNs in normocholesterolemic mice, where they may induce immunologic tolerance.[13] Consistent with this report, we found that UVB irradiation reduced the number of LCs in the epidermis (Figure VIA in the online-only Data Supplement) and concomitantly increased their number in the skin-draining LNs (Figure VIB in the online-only Data Supplement) of hypercholesterolemic mice, implying UVB-mediated emigration of epidermal LCs under hypercholesterolemia.

To specifically evaluate the role of LCs on UVB exposure, we used *Lang-DTR* mice expressing a diphtheria toxin (DT) receptor fused to enhance green fluorescent protein under the control of the *langerin* gene,[17] on an *Apoe*$^{-/-}$ background. Recent studies have identified a population of langerin⁺ DCs in the dermis,[18] which is distinct from LCs in the epidermis although functional differences between these 2 populations have not been fully elucidated. In agreement with the previous report,[18] DT administration to *Lang-DTR*/*Apoe*$^{-/-}$ mice resulted in complete ablation of both dermal langerin⁺ DCs and epidermal LCs on day 2, whereas half of dermal langerin⁺ DCs, but none of epidermal LCs, were recovered on day 9 (Figure 3A), which provided us with the opportunity to assess the role of epidermal LCs in UVB-dependent atheroprotection. To determine the effect of UVB irradiation on CD4⁺Foxp3⁺ Treg responses under LC-depleted conditions, *Lang-DTR*/*Apoe*$^{-/-}$ or *Apoe*$^{-/-}$ mice were intraperitoneally injected with DT on days 0 and 14, irradiated with 5 kJ/m^2 UVB on days 2, 9, and 16, and euthanized on day 20. During this experimental period, near-complete depletion of epidermal LCs was achieved. Notably, UVB irradiation significantly

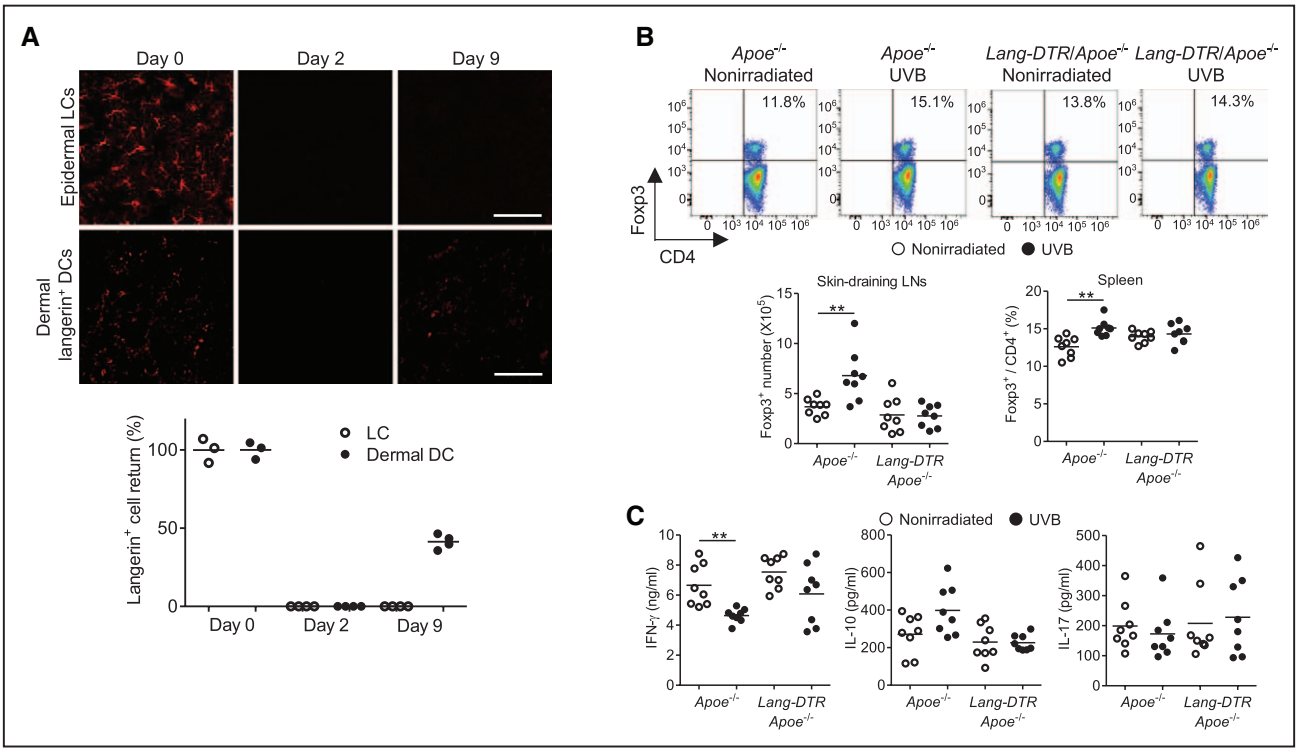

Figure 3. Epidermal Langerhans cells (LCs) are critically involved in UVB-dependent induction of CD4⁺ forkhead box P3 (Foxp3)⁺ regulatory T cells (Tregs) and suppression of proatherogenic T-cell responses. **A**, *Lang-DTR*/apolipoprotein E-deficient (*Apoe*$^{-/-}$) or *Apoe*$^{-/-}$ mice were intraperitoneally injected with diphtheria toxin (DT) on day 0 and euthanized on days 0, 2, and 9. Epidermal and dermal sheets were obtained from these mice, and the density of LCs and dermal langerin⁺ dendritic cells (DCs) was determined. Representative figures and quantitative analyses of epidermal LCs and dermal langerin⁺ DCs detected with an antibody specific for Langerin (red). The graph shows percentage of LC or langerin⁺ DC return. n=3 to 4 per group. White bars represent 100 μm. **B** and **C**, *Lang-DTR*/*Apoe*$^{-/-}$ or *Apoe*$^{-/-}$ mice were intraperitoneally injected with DT on days 0 and 14, irradiated with 5 kJ/m^2 UVB on days 2, 9, and 16, and euthanized on day 20. Nonirradiated mice served as controls. Lymphoid cells from skin-draining lymph nodes (LNs) and spleen were prepared. **B**, Representative results of Foxp3 expression in spleen CD4⁺ T cells assessed by flow cytometry. The graphs represent total numbers of CD4⁺Foxp3⁺ Tregs in LNs and the percentage of Foxp3⁺ Tregs within the spleen CD4⁺ population. n=8 per group. **C**, Splenocytes were prepared and stimulated with concanavalin A in vitro. Cytokine levels in supernatants were examined by ELISA. n=8 per group. Data points represent individual animals. Horizontal bars represent means. $^{**}P<0.01$; Mann–Whitney *U* test.

increased the number of CD4+Foxp3+ Tregs in the skin-draining LNs of DT-treated *Apoe*$^{-/-}$ mice but not of DT-treated *Lang-DTR/Apoe*$^{-/-}$ mice (Figure 3B). Consistently, UVB-mediated increase in the proportion of CD4+Foxp3+ Tregs was not observed in the spleen of LC-depleted mice (Figure 3B). Similar results were obtained for CD4+CD25^{high}Foxp3+ Tregs (Figure VII in the online-only Data Supplement). ELISA analysis revealed that UVB irradiation did not affect IFN-γ, IL-10, or IL-17 production from splenic lymphocytes in LC-depleted mice (Figure 3C), whereas IFN-γ production was inhibited in LC-sufficient mice after UVB irradiation (Figures 2F and 3C). These results collectively suggest that epidermal LCs are indispensable for UVB-mediated CD4+Foxp3+ Treg induction and suppression of proatherogenic T-cell responses in lymphoid organs under hypercholesterolemia.

Epidermal LCs Play a Critical Role in UVB-Dependent Prevention of Intraplaque Accumulation of Inflammatory Cells and Atherosclerosis Development

We further investigated the effect of UVB irradiation on atherosclerosis development under LC-depleted conditions. There was no significant difference in body weight and plasma lipid profile between UVB-irradiated and nonirradiated mice regardless of LC depletion (Table II in the online-only Data Supplement). We found that UVB irradiation did not affect atherosclerotic lesion size in the aortic root (Figure 4A) or intraplaque accumulation of inflammatory cells including macrophages (Figure 4B) and CD4+ T cells (Figure 4C) in DT-treated *Lang-DTR/Apoe*$^{-/-}$ mice, whereas we observed a marked decrease in atherosclerotic lesion formation in UVB-irradiated *Apoe*$^{-/-}$ mice treated with DT (Figure 4A) and UVB-irradiated *Lang-DTR/Apoe*$^{-/-}$ mice treated with PBS (Figure VIII in the online-only Data Supplement) compared with nonirradiated control mice. Moreover, a marked decrease in intraplaque accumulation of inflammatory cells was observed in UVB-irradiated *Apoe*$^{-/-}$ mice treated with DT (Figure 4B and 4C). The number of intraplaque Tregs was not affected by UVB irradiation regardless of LC depletion (data not shown). Taken together, these data demonstrate that epidermal LCs are vital in UVB-mediated atherosclerosis reduction by expanding CD4+Foxp3+ Tregs and suppressing proatherogenic T-cell responses, and suggest that the skin immune system may be an attractive therapeutic target for atherosclerosis.

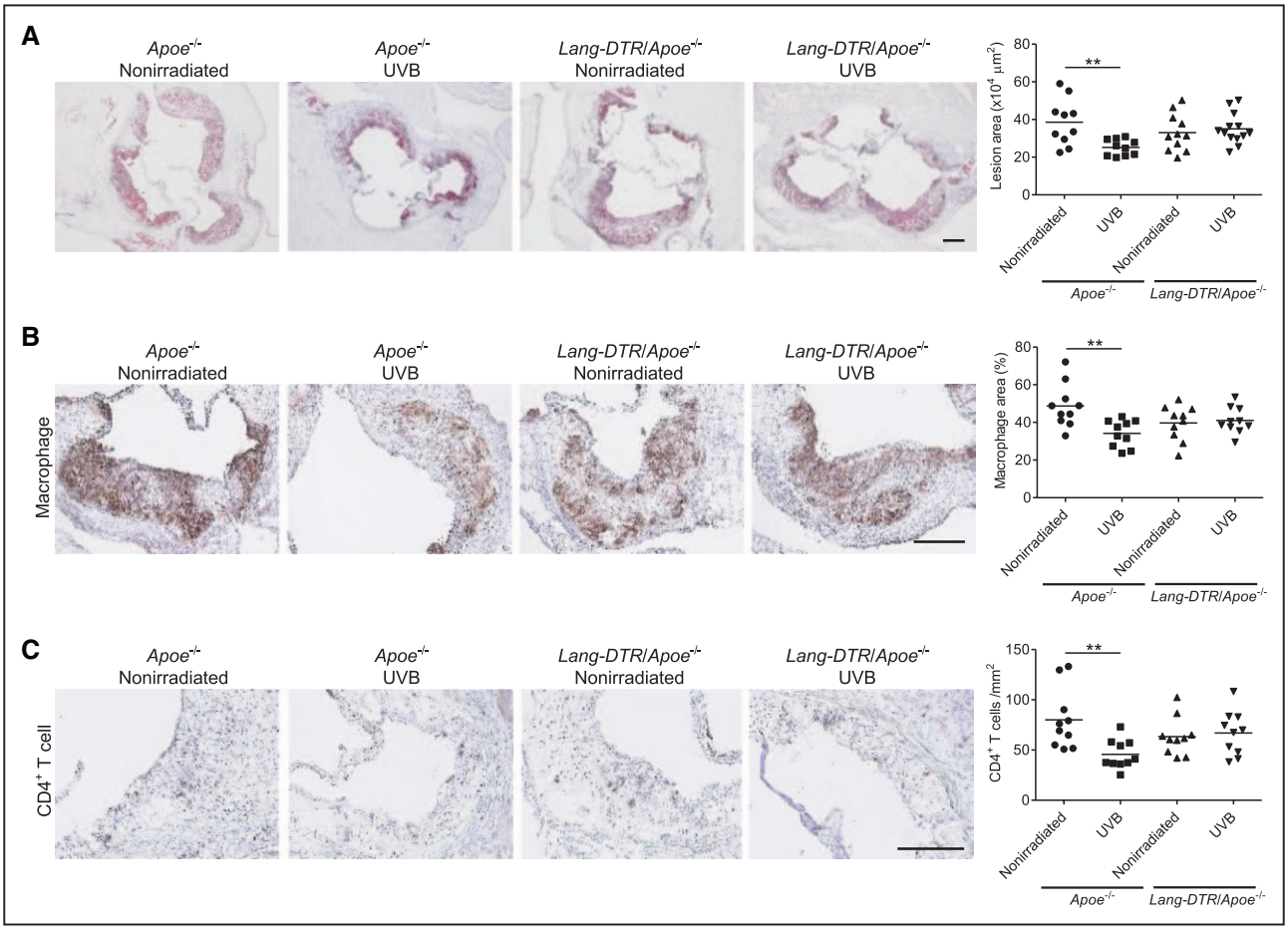

Figure 4. Epidermal Langerhans cells (LCs) play an indispensable role in UVB-dependent reduction of atherosclerosis development and plaque inflammation. Six-wk-old female *Lang-DTR*/apolipoprotein E-deficient (*Apoe*$^{-/-}$) or *Apoe*$^{-/-}$ mice were irradiated with 5 kJ/m^2 UVB once weekly for 14 wk, received intraperitoneal injections of diphtheria toxin every 2 wk and were euthanized at 20 wk of age. Nonirradiated mice served as controls. **A**, Representative photomicrographs of Oil-red-O staining and quantitative analysis of atherosclerotic lesion area in the aortic sinus. n=10 to 13 per group. **B** and **C**, Representative staining and quantitative analyses of MOMA-2+ macrophages (**B**) and CD4+ T cells (**C**). n=10 per group. Data points represent individual animals. Horizontal bars represent means. Black bars represent 200 μm. **P<0.01; Mann–Whitney U test.

Discussion

Although compelling evidence suggests that chronic immunoinflammatory responses are deeply involved in the pathogenesis of atherosclerosis, we have no therapeutics aimed to intervene inflammation or immune system in clinical practice. In the current study, we demonstrate that UVB exposure prevents atherosclerosis by enhancing a regulatory immune response and suppressing proatherogenic immune responses in hypercholesterolemic mice. Experimental studies in LC-depleted mice clearly demonstrated that induction of atheroprotective CD4$^+$Foxp3$^+$ Tregs by UVB-mediated modulation of epidermal LC function is critical for prevention of atherosclerosis, suggesting the skin immune system as a novel therapeutic target for atherosclerosis (Figure IV in the online-only Data Supplement).

Epidemiological studies have suggested a possible link between cardiovascular disease and sunlight exposure.[19–21] One possible explanation for this phenomenon may be decreased levels of immunosuppressive vitamin D.[22] In addition to inadequate dietary intake of vitamin D, limited sunlight exposure is one of the major causes of low vitamin D levels because UVB plays an important role in cutaneous synthesis of vitamin D. Notably, a recent epidemiological study has shown a relationship between low plasma levels of vitamin D and a predisposition to cardiovascular events.[23] Our recent experimental study has demonstrated that oral administration of active form of vitamin D decreases atherosclerosis in hypercholesterolemic mice by promoting induction of tolerogenic DCs and CD4$^+$Foxp3$^+$ Tregs.[24] These studies suggest the possibility that increased plasma levels of vitamin D may contribute to the expansion of Tregs and reduction of atherosclerosis development after UVB exposure. Despite increased plasma levels of biologically active vitamin D (Table II in the online-only Data Supplement), UVB-mediated atheroprotective effects were abrogated on LC depletion, excluding a substantial contribution of increased plasma vitamin D levels to atherosclerosis reduction in our model. Thus, we identified a novel mechanism for UVB-dependent atheroprotection although the differences in its metabolism and atheroprotective properties between mice and humans remain unclear and further clarification is required. However, we cannot exclude that increased local vitamin D levels in the skin might influence LC function and be involved in UVB-dependent induction of CD4$^+$Foxp3$^+$ Tregs and prevention of atherosclerosis development because 1,25-dihydroxyvitamin D is reported to be a strong inducer of receptor activator of nuclear factor-κB ligand,[25] which might be important for UVB-dependent CD4$^+$Foxp3$^+$ Treg induction in the skin.[26]

Inflammation in the arterial wall is an important hallmark of atherosclerosis. Innate and adaptive immunities have been shown to substantially contribute to driving inflammation involved in the pathogenesis of atherosclerosis. Although critical antigens responsible for driving atherosclerosis remain unclear, naive T cells differentiate into effector T cells including the Th1, Th2, and Th17 lineage after antigen presentation by antigen-presenting cells such as DCs. Th1-mediated immune responses such as production of inflammatory cytokine IFN-γ are known to drive atherosclerosis, whereas the roles of Th2 or Th17-mediated immune responses may vary depending on their producing cytokines or animal model used and are still controversial.[2] UVB irradiation has been shown to suppress cutaneous and systemic inflammatory diseases by modulating Th1 and Th2 immune responses, which may vary depending on disease models used.[27–29] Here, we provide first evidence that proatherogenic Th1 immune responses were specifically suppressed after UVB irradiation in hypercholesterolemic mice, in association with marked expansion of activated CD4$^+$Foxp3$^+$ Tregs, whereas Th2 and Th17 immune responses were not affected. Our data suggest that UVB-dependent favorable modulation of the balance between proatherogenic T cells and atheroprotective Tregs may substantially contribute to the prevention of atherosclerosis. We found that expansion of polyclonal-activated CD4$^+$Foxp3$^+$ Tregs are effective enough to prevent proatherogenic immune responses and atherosclerosis development. Given that topical application of haptens onto UVB-exposed skin induces hapten-specific Tregs and inhibit contact hypersensitivity,[28] it is intriguing to speculate that development of antigen-specific Tregs using this method may be more efficacious in preventing atherosclerosis. We expect that such tolerance-inducing therapy could be an attractive approach for the treatment of atherosclerosis not only in mice but also in humans, avoiding unwanted general immunosuppression. To accomplish this, future work should clarify the true antigens responsible for driving atherosclerosis although some antigens have already been shown to be involved in the pathogenesis of experimental atherosclerosis.

DCs are a heterogeneous group of professional antigen-presenting cells involved in induction of immune responses and immune tolerance. Skin-resident DCs are divided into several groups including epidermal LCs and langerin$^+$ or langerin$^-$ dermal DCs.[30] Recent evidence suggests that LCs not only induces adaptive immune responses against invading pathogens but also maintains immune tolerance.[30] Using hypercholesterolemic LC-depleted mice, we have clearly shown that epidermal LCs are critical for UVB-mediated CD4$^+$Foxp3$^+$ Treg induction and suppression of proatherogenic T-cell responses under hypercholesterolemia. However, we cannot exclude that other DC subsets such as CD8α$^+$ DCs might also be involved in UVB-mediated atheroprotective effects because some of these DCs express langerin and are depleted in this mouse model.[17] Receptor activator of nuclear factor -κB ligand is expressed in keratinocytes of the skin and is crucial for the peripheral homeostasis of CD4$^+$CD25$^+$Foxp3$^+$ Tregs by regulating the function of epidermal LCs.[26] UVB exposure induces acute inflammation and DNA damage in the skin,[10,31] which causes activation of epidermal LCs through the upregulation of epidermal receptor activator of nuclear factor -κB ligand expression in keratinocytes.[26] Future work examining more detailed molecular mechanisms for UVB-dependent Treg induction will enable us to design novel therapies for atherosclerotic disease through modulating the skin immune system.

UV-based phototherapy and photochemotherapy have been shown to be established treatments for a large number of immunoinflammatory cutaneous disorders including

psoriasis, atopic dermatitis, and cutaneous T-cell lymphoma in humans without severe adverse effects. Recent clinical studies have shown expansion of peripheral $CD4^+CD25^+Foxp3^+$ Tregs in patients with skin autoimmune disease after UVB phototherapy.[32,33] Based on our data and previous studies, we suppose that UVB phototherapy might be beneficial in treating or preventing human atherosclerosis through expansion of $CD4^+Foxp3^+$ Tregs although the role of Tregs in human atherosclerotic disease has not been fully elucidated. Because excessive UVB exposure may have potential hazardous effects such as skin cancer and exacerbation of infectious diseases, careful management is required for application in clinical settings.

In conclusion, we show that UVB exposure prevents atherosclerosis by expanding and enhancing the functional capacity of atheroprotective $CD4^+Foxp3^+$ Tregs and suppressing proatherogenic immune responses and provide evidence that epidermal LCs play an important role in these processes. Although we should be cautious with extrapolation of our data to the human system, our findings may provide a novel strategy for the treatment and prevention of atherosclerosis.

Acknowledgments

We would like to thank Satomi Minami for technical assistance, Taro Masaki for help with UVB irradiation, and Naoki Kitano for critical reading of the article.

Sources of Funding

This work was supported by JSPS KAKENHI Grant Number 23790849 (N. Sasaki), 25860601 (N. Sasaki), and 24591114 (T. Yamashita), Japan Heart Foundation and Astellas/Pfizer Grant for Research on Atherosclerosis Update (N. Sasaki), Kimura Memorial Heart Foundation Research Grant for 2011 (N. Sasaki), Japan Heart Foundation/Novartis Grant for Research Award on Molecular and Cellular Cardiology 2012 (N. Sasaki), and research grants from the Global Center of Excellence (K. Kasahara), Banyu Life Science Foundation International (N. Sasaki), Suzuken Memorial Foundation (N. S.), ONO Medical Research Foundation (N. Sasaki), Takeda Scientific Foundation (N. Sasaki and T. Yamashita), Senshin Medical Research Foundation (T. Yamashita), Mitsui Life Social Welfare Foundation (T. Yamashita), Yakult Bioscience Research Foundation (T. Yamashita), Uehara Memorial Foundation (K. Hirata), and The Japan Circulation Society Translational Research Foundation (K. Hirata).

Disclosures

None.

References

1. Libby P, Ridker PM, Hansson GK. Progress and challenges in translating the biology of atherosclerosis. *Nature*. 2011;473:317–325. doi: 10.1038/nature10146.
2. Hansson GK, Hermansson A. The immune system in atherosclerosis. *Nat Immunol*. 2011;12:204–212. doi: 10.1038/ni.2001.
3. Sakaguchi S, Yamaguchi T, Nomura T, Ono M. Regulatory T cells and immune tolerance. *Cell*. 2008;133:775–787. doi: 10.1016/j.cell.2008.05.009.
4. Ait-Oufella H, Salomon BL, Potteaux S, Robertson AK, Gourdy P, Zoll J, Merval R, Esposito B, Cohen JL, Fisson S, Flavell RA, Hansson GK, Klatzmann D, Tedgui A, Mallat Z. Natural regulatory T cells control the development of atherosclerosis in mice. *Nat Med*. 2006;12:178–180. doi: 10.1038/nm1343.
5. Sasaki N, Yamashita T, Takeda M, Shinohara M, Nakajima K, Tawa H, Usui T, Hirata K. Oral anti-CD3 antibody treatment induces regulatory T cells and inhibits the development of atherosclerosis in mice. *Circulation*. 2009;120:1996–2005. doi: 10.1161/CIRCULATIONAHA.109.863431.
6. Klingenberg R, Gerdes N, Badeau RM, et al. Depletion of FOXP3+ regulatory T cells promotes hypercholesterolemia and atherosclerosis. *J Clin Invest*. 2013;123:1323–1334. doi: 10.1172/JCI63891.
7. Sasaki N, Yamashita T, Kasahara K, Takeda M, Hirata K. Regulatory T cells and tolerogenic dendritic cells as critical immune modulators in atherogenesis. *Curr Pharm Des*. 2015;21:1107–1117.
8. Wigren M, Björkbacka H, Andersson L, Ljungcrantz I, Fredrikson GN, Persson M, Bryngelsson C, Hedblad B, Nilsson J. Low levels of circulating CD4+FoxP3+ T cells are associated with an increased risk for development of myocardial infarction but not for stroke. *Arterioscler Thromb Vasc Biol*. 2012;32:2000–2004. doi: 10.1161/ATVBAHA.112.251579.
9. Emoto T, Sasaki N, Yamashita T, Kasahara K, Yodoi K, Sasaki Y, Matsumoto T, Mizoguchi T, Hirata K. Regulatory/effector T-cell ratio is reduced in coronary artery disease. *Circ J*. 2014;78:2935–2941.
10. Schwarz T. Mechanisms of UV-induced immunosuppression. *Keio J Med*. 2005;54:165–171.
11. Kripke ML. Immunological unresponsiveness induced by ultraviolet radiation. *Immunol Rev*. 1984;80:87–102.
12. Stingl G, Tamaki K, Katz SI. Origin and function of epidermal Langerhans cells. *Immunol Rev*. 1980;53:149–174.
13. Fukunaga A, Khaskhely NM, Ma Y, Sreevidya CS, Taguchi K, Nishigori C, Ullrich SE. Langerhans cells serve as immunoregulatory cells by activating NKT cells. *J Immunol*. 2010;185:4633–4640. doi: 10.4049/jimmunol.1000246.
14. Schwarz A, Noordegraaf M, Maeda A, Torii K, Clausen BE, Schwarz T. Langerhans cells are required for UVR-induced immunosuppression. *J Invest Dermatol*. 2010;130:1419–1427. doi: 10.1038/jid.2009.429.
15. Lapolla W, Yentzer BA, Bagel J, Halvorson CR, Feldman SR. A review of phototherapy protocols for psoriasis treatment. *J Am Acad Dermatol*. 2011;64:936–949. doi: 10.1016/j.jaad.2009.12.054.
16. Wing K, Onishi Y, Prieto-Martin P, Yamaguchi T, Miyara M, Fehervari Z, Nomura T, Sakaguchi S. CTLA-4 control over Foxp3+ regulatory T cell function. *Science*. 2008;322:271–275. doi: 10.1126/science.1160062.
17. Kissenpfennig A, Henri S, Dubois B, Laplace-Builhé C, Perrin P, Romani N, Tripp CH, Douillard P, Leserman L, Kaiserlian D, Saeland S, Davoust J, Malissen B. Dynamics and function of Langerhans cells in vivo: dermal dendritic cells colonize lymph node areas distinct from slower migrating Langerhans cells. *Immunity*. 2005;22:643–654. doi: 10.1016/j.immuni.2005.04.004.
18. Bursch LS, Wang L, Igyarto B, Kissenpfennig A, Malissen B, Kaplan DH, Hogquist KA. Identification of a novel population of Langerin+ dendritic cells. *J Exp Med*. 2007;204:3147–3156. doi: 10.1084/jem.20071966.
19. Voors AW, Johnson WD. Altitude and arteriosclerotic heart disease mortality in white residents of 99 of the 100 largest cities in the United States. *J Chronic Dis*. 1979;32:157–162.
20. Scragg R. Seasonality of cardiovascular disease mortality and the possible protective effect of ultra-violet radiation. *Int J Epidemiol*. 1981;10:337–341.
21. Grimes DS, Hindle E, Dyer T. Sunlight, cholesterol and coronary heart disease. *QJM*. 1996;89:579–589.
22. Norman PE, Powell JT. Vitamin D and cardiovascular disease. *Circ Res*. 2014;114:379–393. doi: 10.1161/CIRCRESAHA.113.301241.
23. Wang TJ, Pencina MJ, Booth SL, Jacques PF, Ingelsson E, Lanier K, Benjamin EJ, D'Agostino RB, Wolf M, Vasan RS. Vitamin D deficiency and risk of cardiovascular disease. *Circulation*. 2008;117:503–511. doi: 10.1161/CIRCULATIONAHA.107.706127.
24. Takeda M, Yamashita T, Sasaki N, Nakajima K, Kita T, Shinohara M, Ishida T, Hirata K. Oral administration of an active form of vitamin D3 (calcitriol) decreases atherosclerosis in mice by inducing regulatory T cells and immature dendritic cells with tolerogenic functions. *Arterioscler Thromb Vasc Biol*. 2010;30:2495–2503. doi: 10.1161/ATVBAHA.110.215459.
25. Kim S, Yamazaki M, Zella LA, Meyer MB, Fretz JA, Shevde NK, Pike JW. Multiple enhancer regions located at significant distances upstream of the transcriptional start site mediate RANKL gene expression in response to 1,25-dihydroxyvitamin D3. *J Steroid Biochem Mol Biol*. 2007;103:430–434. doi: 10.1016/j.jsbmb.2006.12.020.
26. Loser K, Mehling A, Loeser S, Apelt J, Kuhn A, Grabbe S, Schwarz T, Penninger JM, Beissert S. Epidermal RANKL controls regulatory T-cell numbers via activation of dendritic cells. *Nat Med*. 2006;12:1372–1379. doi: 10.1038/nm1518.
27. Araneo BA, Dowell T, Moon HB, Daynes RA. Regulation of murine lymphokine production in vivo. Ultraviolet radiation exposure depresses IL-2 and enhances IL-4 production by T cells through an IL-1-dependent mechanism. *J Immunol*. 1989;143:1737–1744.

28. Shreedhar VK, Pride MW, Sun Y, Kripke ML, Strickland FM. Origin and characteristics of ultraviolet-B radiation-induced suppressor T lymphocytes. *J Immunol*. 1998;161:1327–1335.
29. Van Loveren H, Boonstra A, Van Dijk M, Fluitman A, Savelkoul HF, Garssen J. UV exposure alters respiratory allergic responses in mice. *Photochem Photobiol*. 2000;72:253–259.
30. Kaplan DH. *In vivo* function of Langerhans cells and dermal dendritic cells. *Trends Immunol*. 2010;31:446–451. doi: 10.1016/j.it.2010.08.006.
31. Nishigori C, Yarosh DB, Ullrich SE, Vink AA, Bucana CD, Roza L, Kripke ML. Evidence that DNA damage triggers interleukin 10 cytokine production in UV-irradiated murine keratinocytes. *Proc Natl Acad Sci U S A*. 1996;93:10354–10359.
32. Furuhashi T, Saito C, Torii K, Nishida E, Yamazaki S, Morita A. Photo(chemo)therapy reduces circulating Th17 cells and restores circulating regulatory T cells in psoriasis. *PLoS One*. 2013;8:e54895. doi: 10.1371/journal.pone.0054895.
33. Iyama S, Murase K, Sato T, et al. Narrowband ultraviolet B phototherapy ameliorates acute graft-versus-host disease by a mechanism involving *in vivo* expansion of CD4+CD25+Foxp3+ regulatory T cells. *Int J Hematol*. 2014;99:471–476. doi: 10.1007/s12185-014-1530-1.

Highlights

- UVB irradiation is known to suppress cutaneous and systemic inflammatory diseases through modulation of the adaptive immune response.
- UVB exposure inhibits the development and progression of atherosclerosis in atherosclerosis-prone mice.
- UVB exposure expands and enhances the functional capacity of atheroprotective $CD4^+Foxp3^+$ regulatory T cells and regulates proatherogenic immune responses.
- Our data may provide a novel strategy for the treatment and prevention of atherosclerosis.

Arteriosclerosis, Thrombosis, and Vascular Biology

JOURNAL OF THE AMERICAN HEART ASSOCIATION

UVB Exposure Prevents Atherosclerosis by Regulating Immunoinflammatory Responses

Naoto Sasaki, Tomoya Yamashita, Kazuyuki Kasahara, Atsushi Fukunaga, Tomoyuki Yamaguchi, Takuo Emoto, Keiko Yodoi, Takuya Matsumoto, Kenji Nakajima, Tomoyuki Kita, Masafumi Takeda, Taiji Mizoguchi, Tomohiro Hayashi, Yoshihiro Sasaki, Mayumi Hatakeyama, Kumiko Taguchi, Ken Washio, Shimon Sakaguchi, Bernard Malissen, Chikako Nishigori and Ken-ichi Hirata

Arterioscler Thromb Vasc Biol. 2017;37:66-74; originally published online October 20, 2016;
doi: 10.1161/ATVBAHA.116.308063
Arteriosclerosis, Thrombosis, and Vascular Biology is published by the American Heart Association, 7272 Greenville Avenue, Dallas, TX 75231

Print ISSN: 1079-5642. Online ISSN: 1524-4636

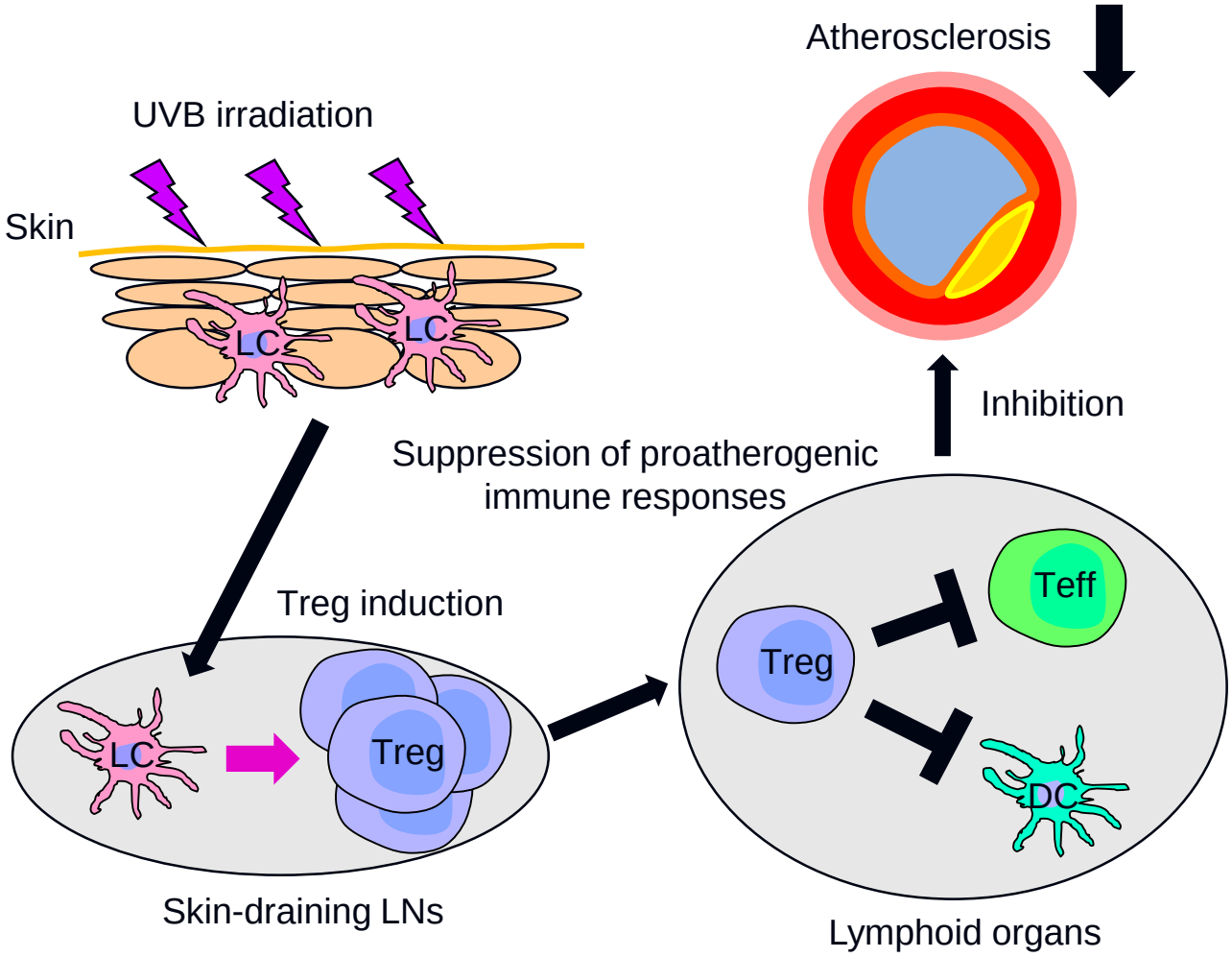
Atherosclerosis
UVB irradiation
Skin
LC
LC
Inhibition
Suppression of proatherogenic
immune responses
Treg induction
Teff
Treg
LC
Treg
DC
Skin-draining LNs
Lymphoid organs

Supplemental Figure I

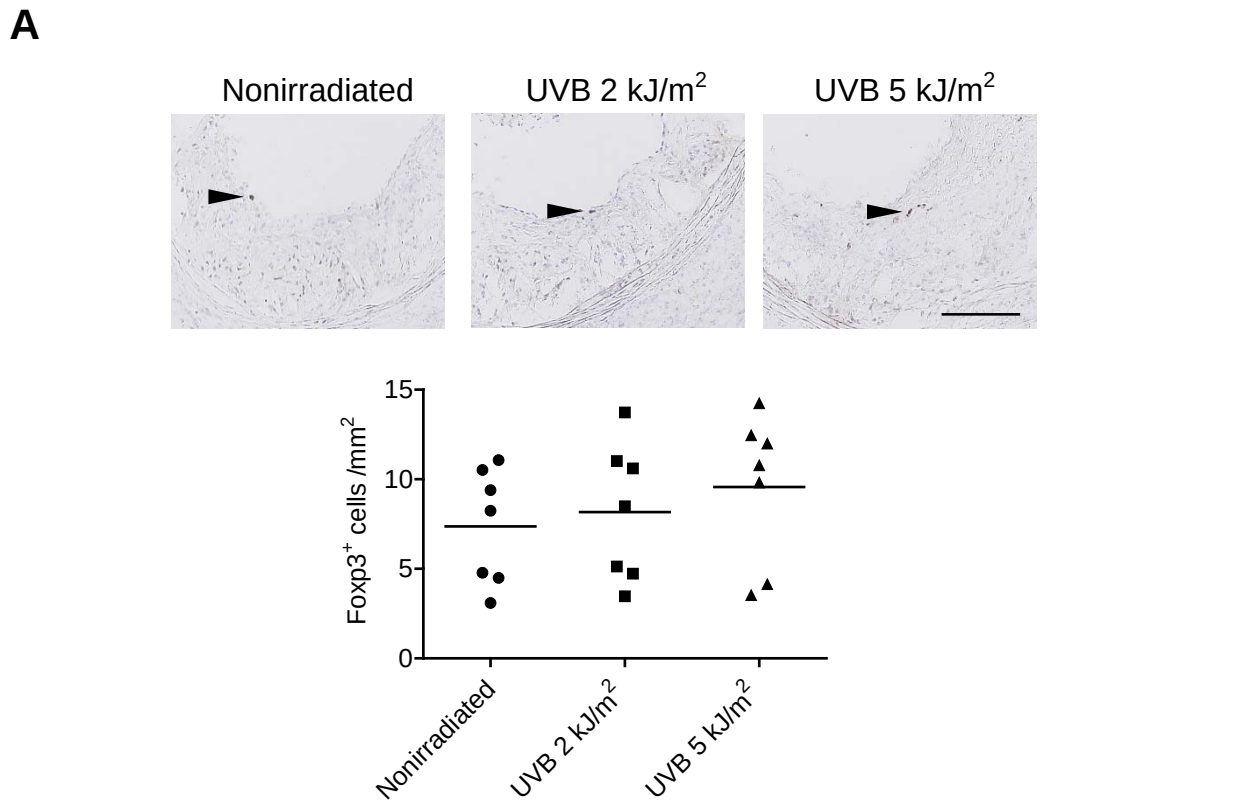

Supplemental Figure I. The effects of UVB irradiation on regulatory T cell (Treg) responses in atherosclerotic plaques. **A**, Representative staining and quantitative analysis of forkhead box P3 (Foxp3)$^+$ cells in the aortic sinus plaques of 20-week-old UVB-irradiated or nonirradiated mice. The black bar represents 100 μm. Arrowheads indicate the Foxp3$^+$ cells. n=7 per group. **B**, Total RNA was extracted from aortas of 20-week-old UVB-irradiated or nonirradiated mice. Expression of Treg-associated markers (Foxp3, cytotoxic T lymphocyte-associated antigen-4 (CTLA-4), CD25, and IL-10) in atherosclerotic aortas was quantified by quantitative real-time reverse transcription PCR and normalized to GAPDH. n=5 to 6 per group. Data points represent individual animals. Horizontal bars represent means. *P<0.05, Mann-Whitney U test.

Supplemental Figure II

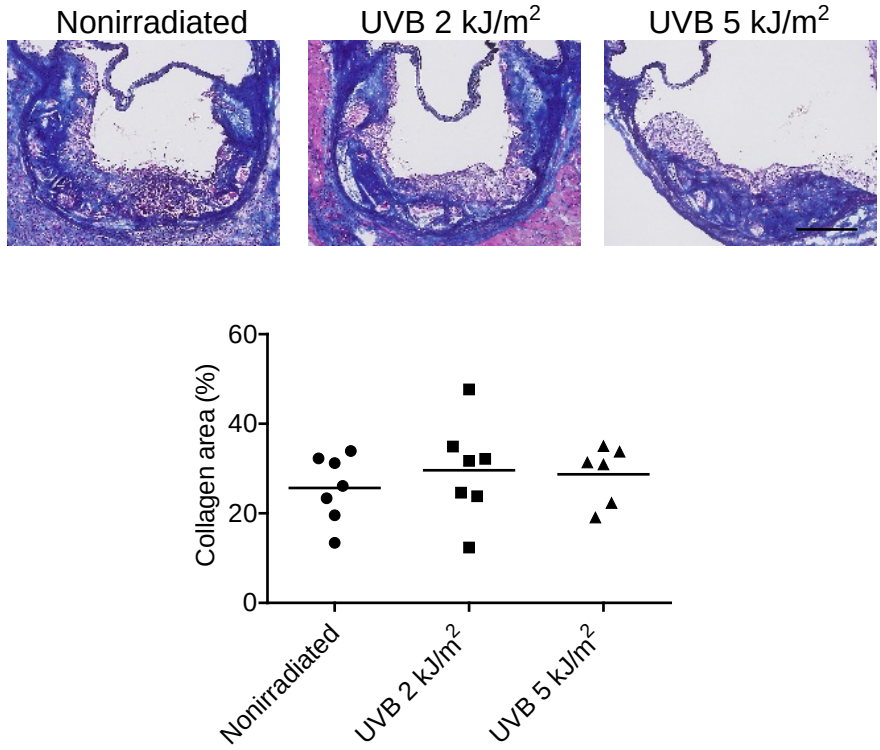

Supplemental Figure II. The effects of UVB irradiation on collagen content in atherosclerotic plaques. Representative staining and quantitative analysis of collagen in the aortic sinus plaques of 20-week-old UVB-irradiated or nonirradiated mice. The black bar represents 200 μm. n= 6 to 7 per group. Data points represent individual animals. Horizontal bars represent means.

Supplemental Figure III

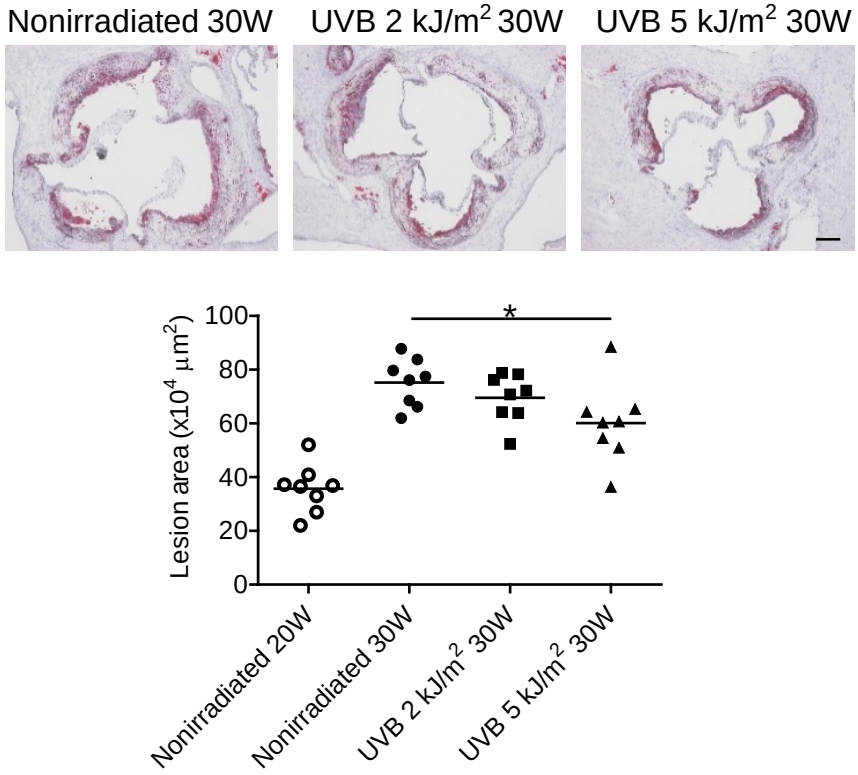

Supplemental Figure III. UVB irradiation suppresses atherosclerotic plaque progression. Twenty-week-old female apolipoprotein E-deficient (*Apoe*$^{-/-}$) mice were irradiated with 2 kJ/m^2 or 5 kJ/m^2 UVB once weekly for 10 weeks and euthanized at 30 weeks of age, and atherosclerotic lesions were assessed. Nonirradiated mice served as controls. Control nonirradiated mice were also euthanized at 20 weeks of age for evaluation of atherosclerotic lesions. Representative photomicrographs of Oil Red O staining and quantitative analysis of atherosclerotic lesion area in the aortic sinus. n=8 per group. The black bar represents 200 µm. Data points represent individual animals. Horizontal bars represent means. *P<0.05, Mann-Whitney U test.

Supplemental Figure IV

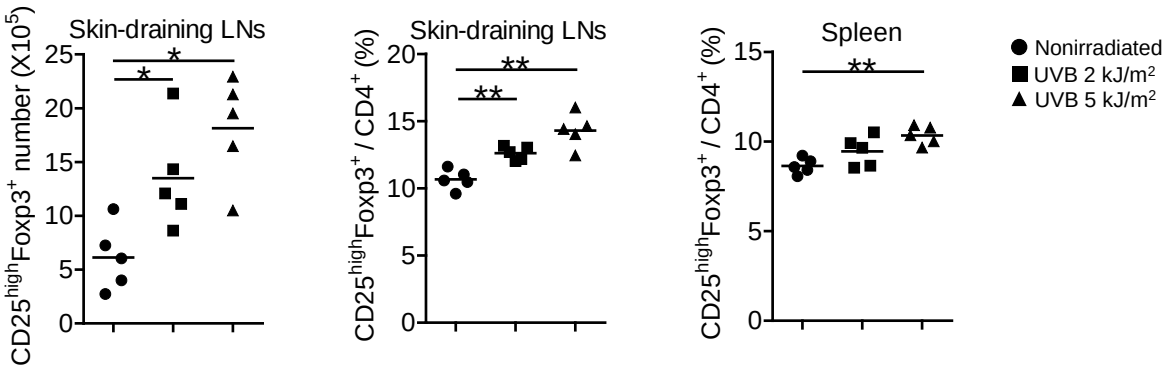

Supplemental Figure IV. UVB irradiation expands $CD4^+CD25^{high}$ forkhead box P3 (Foxp3)$^+$ regulatory T cells (Tregs). Apolipoprotein E-deficient (*Apoe*$^{-/-}$) mice were irradiated with 2 kJ/m^2 or 5 kJ/m^2 UVB once weekly for 3 weeks. Nonirradiated mice served as controls. Three days after the last UVB irradiation, lymphoid cells from skin-draining lymph nodes (LNs) and spleen were prepared. The graphs represent total numbers of LN $CD4^+CD25^{high}Foxp3^+$ Tregs and percentage of $CD4^+CD25^{high}Foxp3^+$ Tregs within the LN and spleen $CD4^+$ population. n=5 per group. Data points represent individual animals. Horizontal bars represent means. **P*<0.05, ***P*<0.01, Mann-Whitney *U* test.

Supplemental Figure V

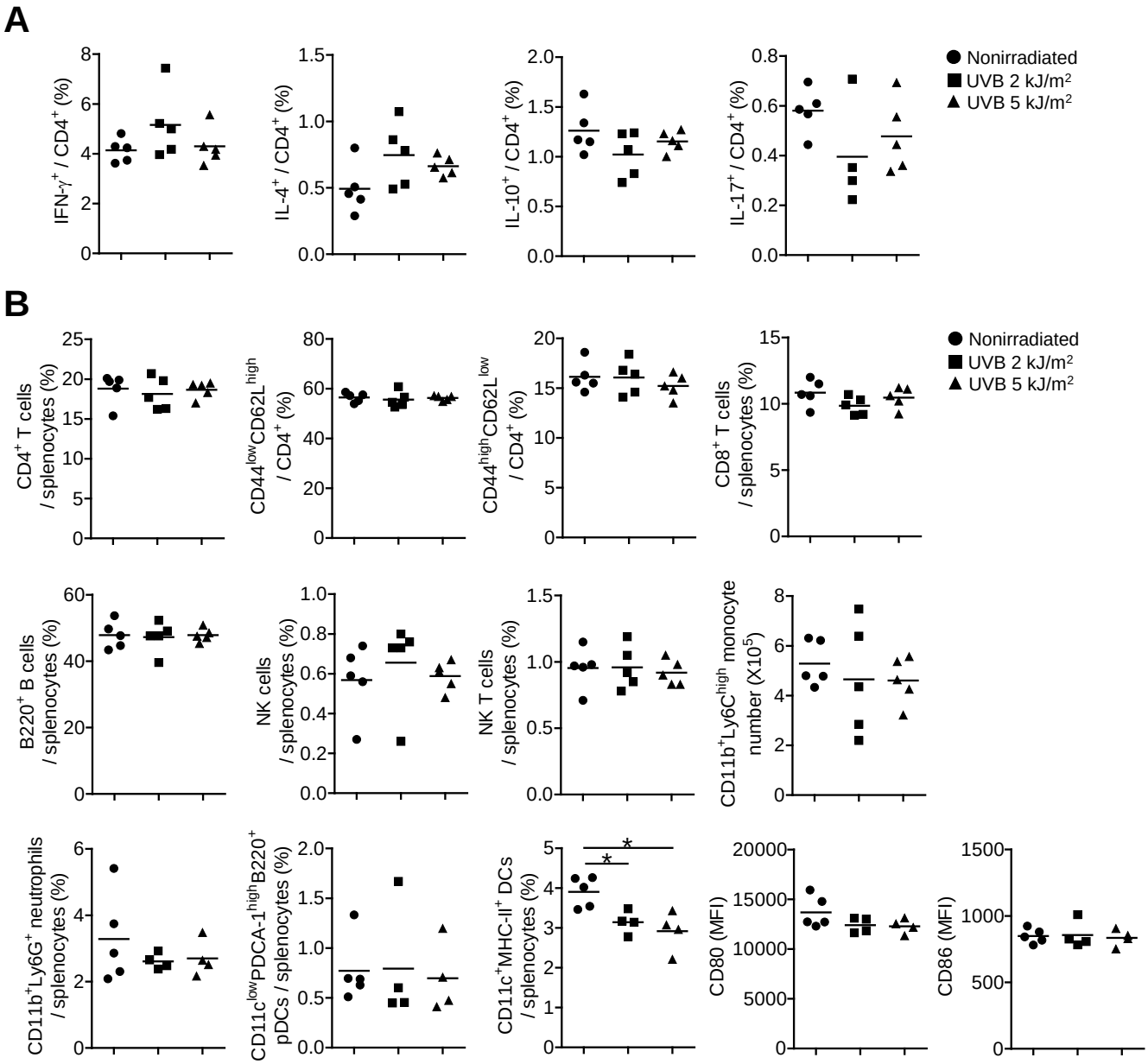

Supplemental Figure V. UVB irradiation does not affect the fractions of helper T cell subsets or immune cells other than $CD4^+$ forkhead box P3 $(Foxp3)^+$ regulatory T cells (Tregs) in the spleen. Apolipoprotein E-deficient (*Apoe*$^{-/-}$) mice were irradiated with 2 kJ/m^2 or 5 kJ/m^2 UVB once weekly for 3 weeks. Nonirradiated mice served as controls. Three days after the last UVB irradiation, lymphoid cells from skin-draining lymph nodes (LNs) and spleen were prepared. **A**, Lymphoid cells from spleen were stimulated with phorbol 12-myristate 13-acetate and ionomycin *in vitro*. Intracellular cytokine staining was performed. The graphs represent the frequencies of interferon (IFN)-γ^+, interleukin (IL)-4^+, IL-10^+, and IL-17^+ $CD4^+$ T cells in the spleen of UVB-irradiated or control mice. n=4 to 5 per group. Data are representative of two independent experiments. **B**, Percentages of splenic $CD4^+$, naïve ($CD44^{low}CD62L^{high}$), effector ($CD44^{high}CD62L^{low}$), and $CD8^+$ T cells, $B220^+$ B cells, natural killer (NK) cells, NKT cells, $CD11b^+Ly6G^+$ neutrophils, $CD11c^{low}PDCA\text{-}1^{high}B220^+$ plasmacytoid dendritic cells (pDCs) and $CD11c^+$ major histocompatibility complex (MHC)-II^+ DCs, CD80 and CD86 expression on $CD11c^+MHC\text{-}II^+$ DCs, and splenic $CD11b^+Ly6C^{high}$ monocyte numbers were determined by flow cytometry. n=4 to 5 per group. Data points represent individual animals. Horizontal bars represent means. $^{**}P<0.05$, Mann-Whitney *U* test. MFI indicates mean fluorescence intensity.

Supplemental Figure VI

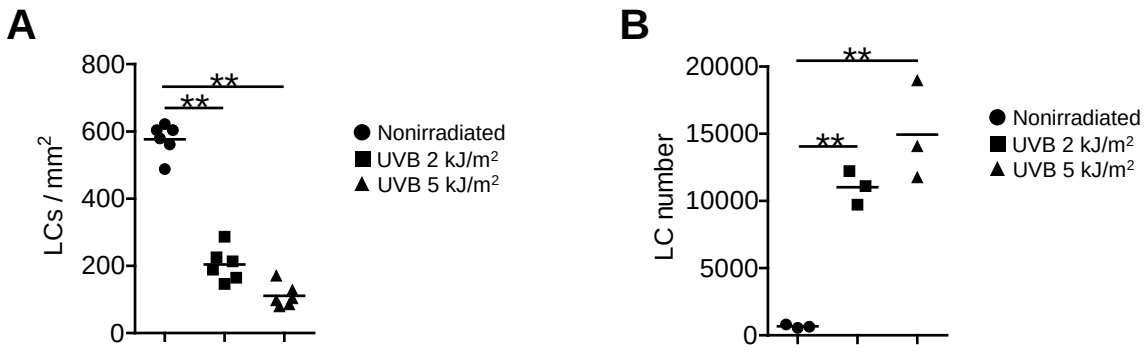

Supplemental Figure VI. Langerhans cells (LCs) migration from the skin to draining lymph nodes (LNs) after UVB irradiation. **A**, Apolipoprotein E-deficient (*Apoe*$^{-/-}$) mice were irradiated with 2 kJ/m^2 or 5 kJ/m^2 UVB. Four days later, epidermal sheets were obtained from UVB-irradiated or nonirradiated mice, and the density of LCs was determined. Quantitative analysis of epidermal LCs detected with an antibody specific for Langerin. n=6 per group. **B**, *Lang-DTR*/*Apoe*$^{-/-}$ mice specifically expressing enhanced green fluorescent protein (eGFP) in langerin$^+$ dendritic cells were irradiated with 2 kJ/m^2 or 5 kJ/m^2 UVB. Seven days later, lymphoid cells from inguinal LNs were prepared, stained for CD11c, CD8α, and CD103, and analyzed for the numbers of LCs using flow cytometry. LCs were defined as GFP$^+$CD11c$^+$CD8α$^-$CD103^{low} cells. The graphs represent total numbers of LCs in the inguinal LNs. n=3 per group. Data points represent individual animals. Horizontal bars represent means. **P<0.01, 2-tailed Student t test.

Supplemental Figure VII

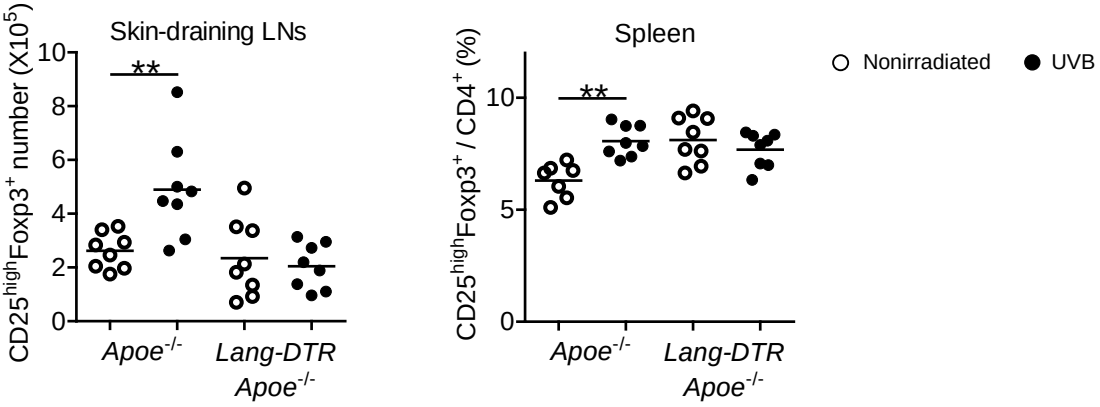

Supplemental Figure VII. Epidermal Langerhans cells (LCs) are critically involved in UVB-dependent induction of $CD4^+CD25^{high}$ forkhead box P3 $(Foxp3)^+$ regulatory T cells (Tregs). *Lang-DTR*/*Apoe*$^{-/-}$ or *Apoe*$^{-/-}$ mice were intraperitoneally injected with diphtheria toxin on days 0 and 14, irradiated with 5 kJ/m^2 UVB on days 2, 9, and 16, and sacrificed on day 20. Nonirradiated mice served as controls. Lymphoid cells from skin-draining lymph nodes (LNs) and spleen were prepared. The graphs represent total numbers of LN $CD4^+CD25^{high}Foxp3^+$ Tregs and percentage of $CD4^+CD25^{high}Foxp3^+$ Tregs within the spleen $CD4^+$ population. n=7 to 8 per group. Data points represent individual animals. Horizontal bars represent means. ***P*<0.01, Mann-Whitney *U* test.

Supplemental Figure VIII

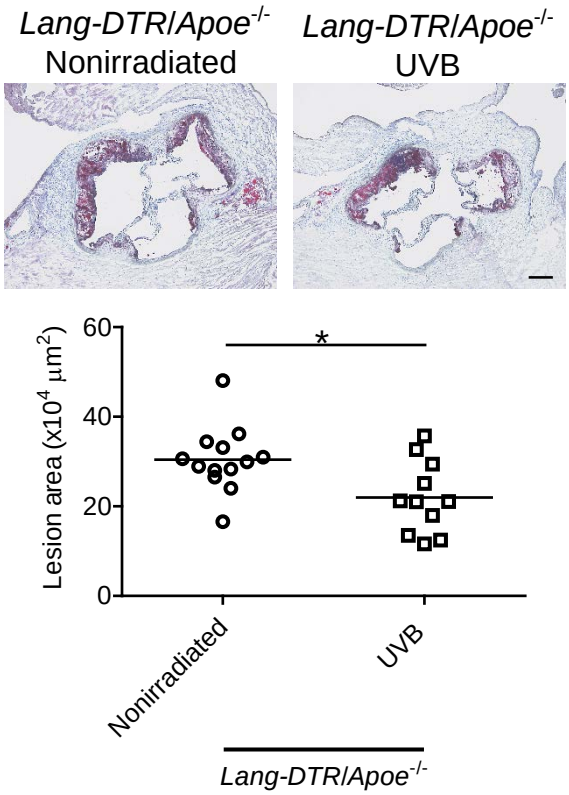

Supplemental Figure VIII. UVB irradiation inhibits atherosclerosis in PBS-treated *Lang-DTR*/apolipoprotein E-deficient (*Apoe*$^{-/-}$) mice. Six-week-old female *Lang-DTR*/*Apoe*$^{-/-}$ mice were irradiated with 5 kJ/m^2 UVB once weekly for 14 weeks, received intraperitoneal injections of PBS every two weeks, and were euthanized at 20 weeks of age. *Lang-DTR*/*Apoe*$^{-/-}$ mice served as controls. Representative photomicrographs of Oil Red O staining and quantitative analysis of atherosclerotic lesion area in the aortic sinus of *Lang-DTR*/*Apoe*$^{-/-}$ mice with or without UVB. n=11 to 13 per group. Data points represent individual animals. Horizontal bars represent means. The black bar represents 200 µm. *P<0.05, Mann-Whitney U test.

Supplemental Figure IV

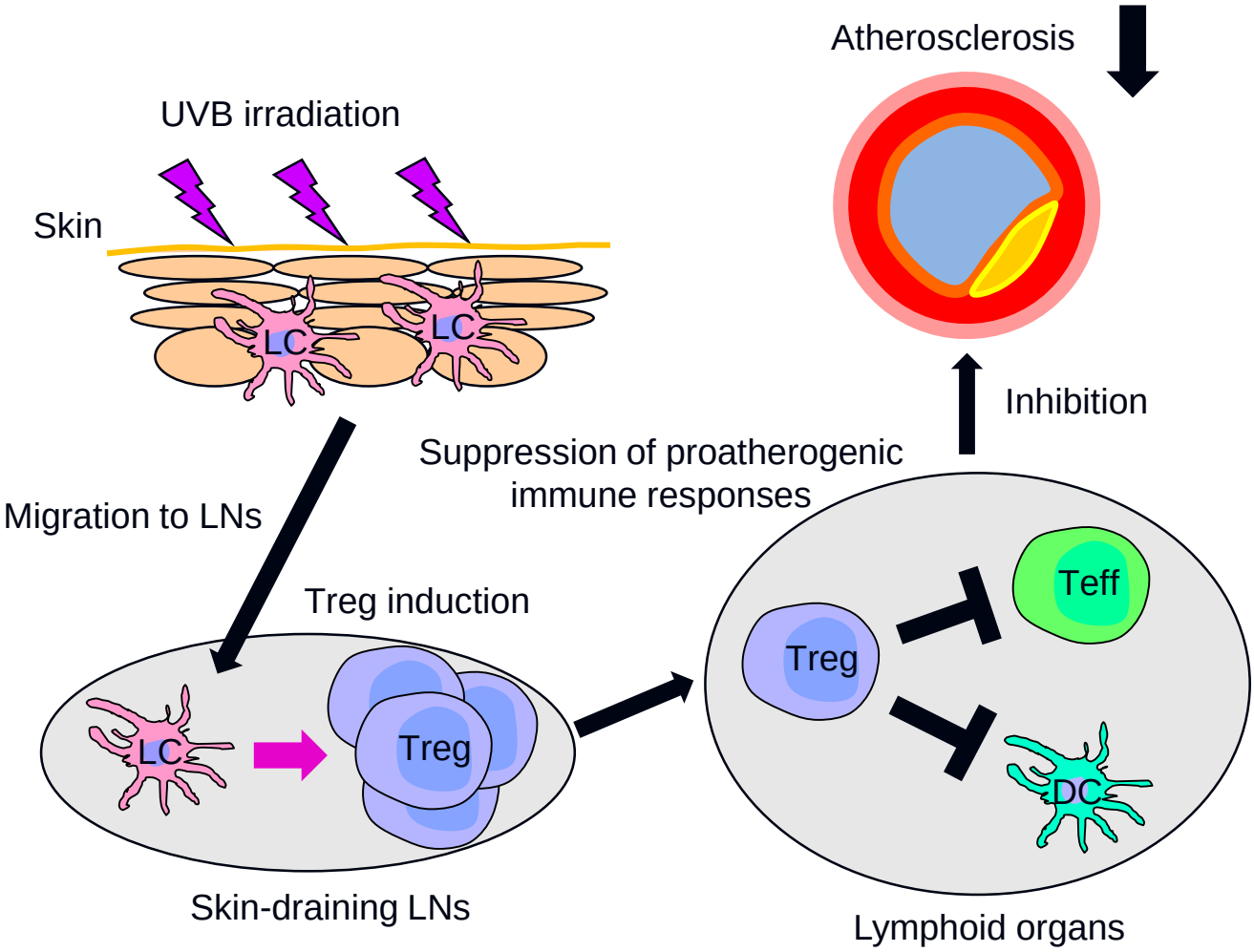

Supplemental Figure IV. Schematic illustrating possible mechanisms of UVB-dependent atheroprotection. UVB exposure activates epidermal Langerhans cells (LCs) which migrate to skin-draining lymph nodes (LNs) and preferentially induce activation and expansion of $CD4^+$ forkhead box P3 $(Foxp3)^+$ regulatory T cells (Tregs). These UVB-induced Tregs migrate into other lymphoid organs and fine-tune immune responses, which may result in inhibiting accumulation of inflammatory immune cells in other chronically inflamed tissues such as atherosclerotic arteries and consequently reducing atherosclerosis. DC, dendritic cell; Teff, effector T cell.

Supplemental Table I

	Nonirradiated	UVB 2 kJ/m^2	UVB 5 kJ/m^2
Body weight (g)	21.9±2.0 (n=10)	21.5±1.3 (n=11)	21.3±1.3 (n=10)
Total cholesterol (mg/dL)	490.3±150.9 (n=7)	516.6±90.0 (n=7)	536.3±38.6 (n=7)
HDL-cholesterol (mg/dL)	8.3±3.1 (n=7)	8.0±3.1 (n=7)	8.3±1.8 (n=7)
Triglycerides (mg/dL)	42.3±15.4 (n=7)	41.7±6.5 (n=7)	41.4±16.2 (n=7)
1,25-dihydroxyvitamin D (pg/mL)	115.5±34.2 (n=7)	171.5±53.2 (n=7)	219.7±56.8** (n=7)
25-hydroxyvitamin D (ng/mL)	55.0±16.7 (n=5)	58.2±9.3 (n=5)	50.5±9.2 (n=4)

Body weight, plasma lipid profile, and vitamin D levels in 20-week-old UVB-irradiated or nonirradiated apolipoprotein E-deficient mice. All data are expressed as the mean±s.d. ***P*<0.01 vs nonirradiated mice, Mann-Whitney *U* test. HDL indicates high-density lipoprotein.

Supplemental Table II

	Apoe$^{-/-}$ Nonirradiated +DT	*Apoe*$^{-/-}$ UVB +DT	*Lang-DTR*/*Apoe*$^{-/-}$ Nonirradiated +DT	*Lang-DTR*/*Apoe*$^{-/-}$ UVB +DT
Body weight (g)	21.2±2.8 (n=10)	20.0±1.0 (n=10)	20.1±2.3 (n=11)	21.1±2.3 (n=13)
Total cholesterol (mg/dL)	550.1±135.7 (n=7)	582.9±110.4 (n=9)	535.6±90.0 (n=11)	559.8±141.3 (n=13)
HDL-cholesterol (mg/dL)	9.3±4.2 (n=7)	6.2±1.6 (n=9)	5.8±2.0 (n=11)	7.7±5.1 (n=13)
Triglycerides (mg/dL)	40.4±13.4 (n=7)	51.7±21.9 (n=9)	35.7±21.6 (n=11)	32.7±11.9 (n=13)
1,25-dihydroxyvitamin D (pg/mL)	93.6±24.4 (n=6)	160.6±55.3** (n=9)	101.4±23.7 (n=7)	223.7±126.3† (n=7)

Body weight, plasma lipid profile, and vitamin D levels in 20-week-old diphtheria toxin (DT)-treated *Langerin-DTR*/apolipoprotein E-deficient (*Apoe*$^{-/-}$) mice and *Apoe*$^{-/-}$ mice with or without UVB exposure for 14 weeks. All data are expressed as the mean±s.d. ***P*<0.01 vs nonirradiated *Apoe*$^{-/-}$ mice, †*P*<0.05 vs nonirradiated *Lang-DTR*/*Apoe*$^{-/-}$ mice, Mann-Whitney *U* test. HDL indicates high-density lipoprotein.

Materials and Methods

UVB Exposure Prevents Atherosclerosis by Regulating Immuno-inflammatory Responses

Naoto Sasaki, Tomoya Yamashita, Kazuyuki Kasahara, Atsushi Fukunaga,
Tomoyuki Yamaguchi, Takuo Emoto, Keiko Yodoi, Takuya Matsumoto,
Kenji Nakajima, Tomoyuki Kita, Masafumi Takeda, Taiji Mizoguchi,
Tomohiro Hayashi, Yoshihiro Sasaki, Mayumi Hatakeyama, Kumiko Taguchi,
Ken Washio, Shimon Sakaguchi, Bernard Malissen,
Chikako Nishigori, Ken-ichi Hirata

Animals

All mice were on a C57BL/6 background and fed normal chow (CLEA, Tokyo, Japan). Apolipoprotein E-deficient (*Apoe*$^{-/-}$) mice are previously described.[1] For *in vivo* depletion of epidermal Langerhans cell (LCs), we used *Lang-DTR* mice[2] and crossed them with *Apoe*$^{-/-}$ mice to obtain *Lang-DTR*/*Apoe*$^{-/-}$ mice. To deplete epidermal LCs, *Lang-DTR*/*Apoe*$^{-/-}$ mice were injected with diphtheria toxin (1 μg/mouse; Sigma) diluted in endotoxin-free PBS. Eight- to twelve-week-old mice were used for all experiments other than atherosclerosis experiments. We housed mice in a specific pathogen-free animal facility at Kobe University, and all animal experiments were conducted according to the Guidelines for Animal Experiments at Kobe University School of Medicine.

UVB irradiation

TL 20W/12RS fluorescent lamps (Philips, Eindhoven, Holland) were used to irradiate the mice with broad-band UVB. TL 20W/12RS lamps emit a continuous spectrum from 275 to 390 nm, with a peak emission at 313 nm; approximately 65% of that radiation is within the UVB wavelength range (280-320 nm). The irradiance was 6.6 J/m^2/second at a distance of 40 cm, as measured by a Digital UV Intensity Meter UIT-250 (USHIO, Tokyo, Japan). The mice were placed 40cm below the bank of lamps and were irradiated for indicated weeks after shaving their backs as previously described.[3]

Assessment of biochemical parameters

After overnight fasting, blood was collected by the cardiac puncture under anesthesia. Plasma was obtained through centrifugation and stored at -80°C until measurement. Concentrations of plasma total cholesterol, high-density lipoprotein-cholesterol, and triglyceride were determined enzymatically using an automated chemistry analyzer (SRL, Tokyo, Japan). 1,25-dihydroxyvitamin D and 25-hydroxyvitamin D were analyzed by radioimmunoassay as described previously.[4]

Atherosclerotic lesion assessment

Mice were anesthetized and the aorta was perfused with saline. The aorta was dissected from the middle of the left ventricle to the bifurcation of the iliac artery. For aortic root lesion analysis, the samples were cut in the ascending aorta, and the proximal samples containing the aortic sinus were embedded in OCT compounds (Tissue-Tek; Sakura Finetek, Tokyo, Japan). Five consecutive sections (10 μm thickness), spanning

550 μm of the aortic sinus, were collected from each mouse and stained with Oil Red O (Sigma) or hematoxylin-eosin. Stained sections were digitally captured using an All-in-one Type Fluorescence Microscope (BZ-8000; Keyence, Osaka, Japan). For quantitative analysis of atherosclerosis, the total lesion area of 5 separate sections from each mouse was obtained with the use of the Image J (National Institutes of Health) as previously described.[1] For en face lesion analysis, the aorta was excised from the proximal ascending aorta to the common iliac artery bifurcation and fixed in 10% buffered formalin. After the adventitial tissue was carefully removed, the aorta was opened longitudinally, stained with Oil Red O, pinned on a black wax surface, and captured digitally with a digital camera. The percentage of stained lesion area per total area of the aorta was determined by Image J as described previously.[1]

Immunohistochemical analysis of atherosclerotic lesions

Immunohistochemistry was performed on acetone-fixed or formalin-fixed cryosections (10 μm) of mouse aortic roots using antibodies to identify macrophages (MOMA-2, 1:400; BMA Biomedicals), T cells (CD4, 1:100; BD Biosciences), and forkhead box P3 $(Foxp3)^+$ regulatory T cells (Tregs) (Foxp3, clone FJK-16s, 1:100; eBioscience), followed by detection with biotinylated secondary antibodies and streptavidin-horseradish peroxidase. The appropriate fixation reagent depending on the primary antibodies was used. Staining with Masson's trichrome was used to delineate the fibrous area. Stained sections were digitally captured using an All-in-one Type Fluorescence Microscope, and the percentage of the stained area (the stained area per total atherosclerotic lesion area) was calculated. Quantification of $CD4^+$ T cells or

Foxp3$^+$ cells was done as described previously[1] by counting positively stained cells, which was divided by total plaque area.

Flow cytometry

For fluorescent-activated cell sorter analysis of lymphoid tissues, skin-draining lymph node (LN) cells and splenocytes were isolated and stained in PBS containing 2% fetal calf serum. We used axillary and inguinal LNs as skin-draining LNs. For detection of LCs in skin-draining LNs, we prepared LN cell suspensions using Librase Blendzyme II (Roche Diagnostics). Flow cytometric analysis was performed by Attune Acoustic Focusing Cytometer (Life Technologies) or FACS Canto II (BD Biosciences) using FlowJo software (Tree Star). The antibodies used were as follows; anti-CD3 (clone 145-2C11; BD Biosciences), anti-CD4 (clone RM4-5; BD Biosciences), anti-CD8 (clone 53-6.7; BD Biosciences), anti-CD25 (clone PC61; BD Biosciences), anti-CD44 (clone IM7; BD Biosciences), anti-CD62L (clone MEL-14; BD Biosciences), anti-CD103 (clone M290; BD Biosciences), anti-GITR (clone DTA1; BD Biosciences), anti-CTLA-4 (clone UC10; BD Biosciences), ani-Foxp3 (clone FJK-16s; eBioscience), anti-CD11b (clone M1/70; BD Biosciences), anti-CD11c (clone HL3; BD Biosciences), anti-CD80 (clone 16-10A1; BD Biosciences), anti-CD86 (clone GL1; BD Biosciences), anti-PDCA-1 (clone927; Biolegend), anti-B220 (clone RA3-6B2; BD Biosciences), anti-NK1.1 (clone PK136; BD Biosciences), anti-Ly6C (clone AL-21; BD Biosciences), anti-Ly6G (clone 1A8; BD Biosciences), anti-IL-4, (clone BVD4-1D11; eBioscience), anti-IL-10 (clone JES5-16E3; eBioscience), anti-IL-17 (clone 17-B7; BD Bioscience), anti-IFN-γ (cloneXMG1.2; eBioscience), and isotype matched control antibodies. Intracellular staining of Foxp3 was performed using the Foxp3 staining buffer set

(eBioscience) according to the manufacturer's instructions. All staining procedure was performed after blocking Fc receptor with anti-CD16/CD32 (clone 2.4G2; BD Bioscience). Surface stainings were performed according to standard procedures at a density of 5-10 x10^5 cells per 50 μL, and volumes were scaled up accordingly.

Cytokine and cell suppression assays

In all cell culture experiments, we used RPMI 1640 medium (Sigma) supplemented with 10% fetal calf serum, 50 μmol/L 2β-mercaptoethanol and antibiotics. For the culture of splenocytes, whole isolated cells were cultured in 24-well plates in RPMI medium at a concentration of 4×10^6 cells/mL and stimulated with 2 μg/mL concanavalin A (Sigma). Culture supernatants were collected at 72 hours and analyzed by ELISA for interleukin (IL)-4, IL-10, IL-17, and interferon-γ using paired antibodies specific for corresponding cytokines according to the manufacturer's instructions (R & D Systems). For analysis of *in vitro* suppressive function, $CD4^+CD25^{high}$ Tregs were purified from skin-draining LNs using a MoFlo cell sorter (DakoCytomation). $CD4^+CD25^-$ responder T cells were purified from spleen of nonirradiated mice using a MoFlo cell sorter. The purity of each population was >98% by flow cytometric analysis. Purified $CD4^+CD25^{high}$ Tregs from UVB-irradiated and control mice were co-cultured with responder $CD4^+CD25^-$ T cells (1×10^4 cells) at the indicated ratios in the presence of irradiated antigen-presenting cells and soluble anti-CD3 antibody (0.5 μg/mL, clone 145-2C11; BD Biosciences) in 96-well round-bottomed plates. The co-cultured cells were maintained at 37°C with 5% CO_2 for 4 days. [^{3}H]-thymidine incorporation during the last 6 to 10 hours of culture was measured.

Flow cytometric analysis of dendritic cell phenotypic changes

$CD4^+CD25^+$ Tregs and $CD4^+CD25^-$ T cells were purified from skin-draining LNs after UVB irradiation using a $CD4^+CD25^+$ Regulatory T Cell Isolation Kit (Miltenyi Biotec) according to the manufacturer's instructions. The purity of each population was >95% by flow cytometric analysis. $CD11c^+$ dendritic cells were isolated by using MACS (Miltenyi Biotec) from spleen of nonirradiated mice treated with Librase Blendzyme II. The purity of $CD11c^+$ population was around 93% by flow cytometric analysis. $CD4^+CD25^-$ T cells (5×10^4 cell) or a mix of $CD4^+CD25^+$ Tregs (5×10^4 cells) and $CD4^+CD25^-$ T cells at a 1:1 ratio were cultured with splenic $CD11c^+$ dendritic cells (2.5×10^4 cells) in the presence of soluble anti-CD3 antibody (0.5 μg/mL) in 96-well round-bottomed plates. After 48 hour co-culture, cells were collected, stained with antibodies specific for CD4, CD11c, CD80, CD86, and 7-amino-actinomycin D, and analyzed using Attune Acoustic Focusing Cytometer.

Intracellular cytokine staining

Splenocytes were stimulated with 20 ng/ml phorbol 12-myristate 13-acetate (Sigma) and 1 mmol/L ionomycin (Sigma) for 5 hours in the presence of GolgiStop (BD Biosciences). After staining for surface antigens, intracellular cytokine staining was performed using an intracellular cytokine staining kit (BD Biosciences) and anti-cytokine antibodies according to the manufacturer's instructions.

Preparation of epidermal and dermal sheets and immunofluorescence analysis

Epidermal or dermal sheets were prepared as described previously.[5] Ears were cut off and incubated with 2 mmol/L NaBr for 2 hours at 37℃. The epidermis was

separated from dermis using forceps and was washed in PBS. Epidermal or dermal sheets were fixed in acetone for 3-5 minutes at -20℃. After fixation, the sheets were washed in PBS and incubated with rat anti-mouse Langerin antibody (clone RMUL.2; eBioscience) in 5% bovine serum albumin/PBS (1:100) at room temperature overnight. After washing with PBS, the sheets were incubated with Alexa Fluor 594 goat anti-rat secondary antibody (Life Technologies) in 5% bovine serum albumin/PBS (1:100) at room temperature for 30 minutes. Finally, the sheets were washed in PBS and mounted upside down with Prolong Gold antifade reagent with DAPI (Life Technologies) on microscope slides. The samples were analyzed using an All-in-one Type Fluorescence Microscope.

Real-time reverse transcription PCR analysis

Total RNA was extracted from aortas after perfusion with RNA later (Life Technologies) using TRIzol reagent (Life Technologies). For RT, a PrimeScript RT reagent Kit (Takara, Shiga, Japan) was used. Quantitative PCR was performed as described previously[6] using a SYBER Premix Ex Taq (Takara) and an ABI PRISM 7500 Sequence Detection system (Life Technologies) according to the manufacturer's protocol. The following primers were used to amplify Foxp3, CTLA-4, CD25, IL-10, and GAPDH: Foxp3, 5'-CTC ATG ATA GTG CCT GTG TCC TCA A-3' and 5'-AGG GCC AGC ATA GGT GCA AG-3'; CTLA-4, 5'-CCT CTG CAA GGT GGA ACT CAT GTA-3' and 5'-AGC TAA CTG CGA CAA GGA TCC AA-3'; CD25, 5'-CTG ATC CCA TGT GCC AGG AA-3' and 5'-AGG GCT TTG AAT GTG GCA TTG-3'; IL-10, 5'-GAC CAG CTG GAC AAC ATA CTG CTA A-3' and 5'-GAT AAG GCT TGG CAA CCC AAG TAA-3'; GAPDH, 5'-TGT GTC CGT CGT GGA TCT GA-3' and 5'-TTG

CTG TTG AAG TCG CAG GAG-3'. Amplification reactions were performed in duplicate and fluorescence curves were analyzed with included software. GAPDH was used as an endogenous control reference.

Statistical analysis

Two-tailed Student *t* test or Mann-Whitney *U* test was used to detect significant differences between 2 groups where appropriate. A value of $P<0.05$ was considered statistically significant.

References

1. Sasaki N, Yamashita T, Takeda M, Shinohara M, Nakajima K, Tawa H, Usui T, Hirata K. Oral anti-CD3 antibody treatment induces regulatory T cells and inhibits the development of atherosclerosis in mice. *Circulation*. 2009;120:1996-2005
2. Kissenpfennig A, Henri S, Dubois B, Laplace-Builhe C, Perrin P, Romani N, Tripp CH, Douillard P, Leserman L, Kaiserlian D, Saeland S, Davoust J, Malissen B. Dynamics and function of Langerhans cells in vivo: Dermal dendritic cells colonize lymph node areas distinct from slower migrating Langerhans cells. *Immunity*. 2005;22:643-654
3. Kunisada M, Kumimoto H, Ishizaki K, Sakumi K, Nakabeppu Y, Nishigori C. Narrow-band UVB induces more carcinogenic skin tumors than broad-band UVB through the formation of cyclobutane pyrimidine dimer. *J Invest Dermatol*. 2007;127:2865-2871

4. Takeda M, Yamashita T, Sasaki N, Nakajima K, Kita T, Shinohara M, Ishida T, Hirata K. Oral administration of an active form of vitamin D3 (calcitriol) decreases atherosclerosis in mice by inducing regulatory T cells and immature dendritic cells with tolerogenic functions. *Arterioscler Thromb Vasc Biol*. 2010;30:2495-2503

5. Fukunaga A, Nagai H, Noguchi T, Okazawa H, Matozaki T, Yu X, Lagenaur CF, Honma N, Ichihashi M, Kasuga M, Nishigori C, Horikawa T. Src homology 2 domain-containing protein tyrosine phosphatase substrate 1 regulates the migration of Langerhans cells from the epidermis to draining lymph nodes. *J Immunol*. 2004;172:4091-4099

6. Kasahara K, Sasaki N, Yamashita T, Kita T, Yodoi K, Sasaki Y, Takeda M, Hirata K. CD3 antibody and IL-2 complex combination therapy inhibits atherosclerosis by augmenting a regulatory immune response. *Journal of the American Heart Association*. 2014;3:e000719

UVB 暴露能够调节炎症免疫反应从而预防动脉粥样硬化

动脉粥样硬化疾病是发达国家主要的死亡原因之一，主要包括缺血性心脏病和脑卒中。动脉粥样硬化中存在动脉管壁的慢性炎症反应。固有免疫和获得性免疫促进了动脉粥样硬化斑块的发展和破裂及血栓性的动脉闭塞，最终导致临床死亡事件的发生。

T 细胞介导的血管慢性炎症反应在动脉粥样硬化的发生中发挥了重要作用。UVB 照射是皮肤炎症免疫失调确定有效的治疗方法，并且能够通过调节获得性免疫应答来抑制皮肤及全身的免疫性疾病。然而，UVB 的照射是否能够预防动脉的炎症免疫性疾病（如动脉粥样

硬化）尚不清楚，近日，有学者对相关问题进行了初步研究，结果发现 UVB 的暴露能够增强 $CD4^+Foxp3^+$调节性 T 细胞的功能及调节促动脉粥样硬化 T 细胞的应答，从而抑制了易感小鼠动脉粥样硬化的发生和发展。利用朗汉斯细胞缺乏小鼠的实验研究发现，表皮朗汉斯细胞在 UVB 依赖的 $CD4^+FOXP3^+$调节性 T 细胞诱导、促动脉粥样硬化 T 细胞应答的抑制以及动脉粥样硬化斑块的预防等功能上发挥了重要作用。

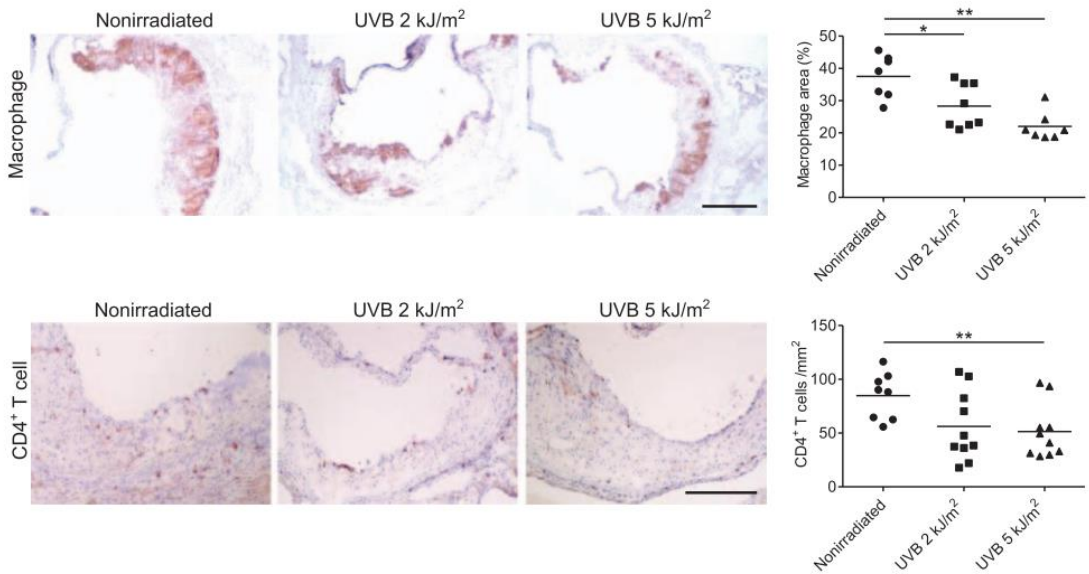

图 UVB 照射对动脉粥样硬化表型的影响

因此，不难看出皮肤免疫系统可能成为一个治疗动脉粥样硬化的新靶点，为动脉粥样硬化疾病的预防和治疗带来了新思路。

（Arterioscler Thromb Vasc Biol. 2017;37:66-74.）